Journal of the Mechanics and Physics of Solids 91 (2016) 334–358

Contents lists available at ScienceDirect

Journal of the Mechanics and Physics of Solids

journal homepage: www.elsevier.com/locate/jmps

Thermomechanical formulation of ductile damage coupled to nonlinear isotropic hardening and multiplicative viscoplasticity

C. Soyarslan [a,*], S. Bargmann [a,b]

[a] Institute of Continuum Mechanics and Material Mechanics, Hamburg University of Technology 21073 Hamburg, Germany
[b] Institute of Materials Research, Helmholtz-Zentrum Geesthacht 21502 Geesthacht, Germany

ARTICLE INFO

Article history:
Received 13 November 2014
Received in revised form
1 March 2016
Accepted 2 March 2016
Available online 5 March 2016

Keywords:
Damage coupled elastoplasticity
Thermomechanical coupling
Finite strain
Finite elements
Numerical algorithms
Return map

ABSTRACT

In this paper, we present a thermomechanical framework which makes use of the internal variable theory of thermodynamics for damage-coupled finite viscoplasticity with nonlinear isotropic hardening. Damage evolution, being an irreversible process, generates heat. In addition to its direct effect on material's strength and stiffness, it causes deterioration of the heat conduction. The formulation, following the footsteps of Simó and Miehe (1992), introduces inelastic entropy as an additional state variable. Given a temperature dependent damage dissipation potential, we show that the evolution of inelastic entropy assumes a split form relating to plastic and damage parts, respectively. The solution of the thermomechanical problem is based on the so-called isothermal split. This allows the use of the model in 2D and 3D example problems involving geometrical imperfection triggered necking in an axisymmetric bar and thermally triggered necking of a 3D rectangular bar.

1. Introduction

Plasticity and damage are two path dependent deformation mechanisms that differ on micro-mechanical foundations. The former entails crystal slip through dislocation movements, while the latter involves the nucleation, growth and coalescence of micro-voids and/or micro-cracks.

In a thermomechanical problem, heat is produced by dissipated mechanical work in addition to external heat sources if any exist. Produced heat is conducted/convected over the problem domain where rate sensitivity is applicable even to rate-independent models due to the time-dependence of heat flux (Wriggers et al., 1992). In order to solve the coupled problem for deformation and temperature one has to take into account a set of complicated mutual interactions among fields. In the absence of damage, problems of interest in thermoplasticity often display a two sided coupling: the influence of the thermal field on the mechanical field (thermal expansion, temperature induced elastic softening with temperature dependence of elastic material properties, temperature induced plastic softening with yield locus shrinkage), the influence of the mechanical field on the thermal field (geometric coupling on heat flux, heat generation by plastic dissipation, structural elastic heating: the Gough–Joule effect.)

In the current context, plasticity and damage account for irreversible dissipative processes. In addition to the ones

* Corresponding author. Tel.: +49(0)40/42878 2562.
E-mail address: celal.soyarslan@tuhh.de (C. Soyarslan).

http://dx.doi.org/10.1016/j.jmps.2016.03.002

mentioned above, conditions that must be analyzed in the presence of damage include the action of damage on the other mechanical fields (damage induced elastic softening with deteriorated elastic stiffness, damage induced plastic softening with yield locus shrinkage), the influence of damage on the thermal field (heat generation by damage dissipation, damage dependent heat flux), and the influence of the thermal field on damage (direct effect through temperature dependence of the damage dissipation functions, indirect effect through reconstruction of other damage driving mechanical fields, e.g., triaxiality).

This highly coupled setting is the norm rather than the exception for many engineering applications. In context of isotropic damage coupled finite plasticity, different numerical models are presented by Simó and Ju (1989), Ju (1990), Steinmann et al. (1994), de Souza Neto and Perić (1995), Lämmer and Tsakmakis (2000), and Andrade Pires et al. (2004), among others. These frameworks, however, are presented in a purely isothermal setting. da Cunda et al. (1998) present a damage coupled finite strain thermoplastic framework utilizing Gurson damage model, whereas Lemaitre damage model is presented in Saanouni and Chaboche (2003). More recently, a combination of Lemaitre and Gurson damage models, for modeling micro-void and/or micro-crack driven failure in metals at finite strains, is presented in Soyarslan et al. (2016). Formulations based on a multiplicative framework are given in Ganapathysubramanian and Zabaras (2003) where a continuum sensitivity method is developed for porous metal plasticity using Gurson damage model. In the mentioned applications, the effect of damage on heat conduction is not reflected. However, at the microscale the deterioration of the material continuity through void nucleation, growth and coalescence inherently affects the conduction quality.

Bracketing anisotropy and reducing the symmetry class to simple isotropy, the current study aims to formulate a consistent thermodynamic framework for finite multiplicative thermoplasticity coupled to damage along the same lines with Simó and Miehe (1992). Accordingly, exploiting the additivity or extensive property of the entropy, its decomposition into elastic and inelastic parts is postulated. It is shown that, together with temperature dependent plastic and damage dissipation potentials, the internal variable inelastic entropy has a natural split into plastic and damage parts. This amounts to a generalization of the postulated results suggested by Simó and Miehe (1992) to the case of damage coupling. Consequently, not only the plastic structural changes due to dislocation and lattice defect motion but also the damage structural changes due to microvoid nucleation, growth and coalescence are consistently linked to their regarding entropies.

A principal axes formulation is used based on a hyperelastic potential quadratic in Hencky strains (Soyarslan et al., 2008). This way, the stress from a properly articulated definition of elastic potential supplies a precise elastic prediction. Besides, hypoelastic stress formulations lead to dissipation for even closed elastic cycles (Weber and Anand, 1990). Nonlinear isotropic hardening von Mises plasticity (which is typical for metals) is used with a Perzyna-type overstress formulation. In resolution of damage, an isotropic Lemaitre damage model is selected, where the effective stress concept (Kachanov, 1958; Rabotnov, 1968), together with strain equivalence principle (Lemaitre, 1971), form the bases.

The paper has the following organization. Section 2 outlines the mathematical theory. Specification of constitutive functions particularly for metals is realized in Section 3. Numerical implementation is discussed in Section 4 where the staggered treatment of the coupled initial boundary value problem as well as local return mapping methodology is summarized. Finally, in Section 5 capabilities of the model are demonstrated through application problems in 2D and 3D including geometrically triggered necking of an axisymmetric bar and thermally triggered necking of a 3D rectangular bar.

2. Mathematical theory

2.1. Fundamental kinematics

Let[1] $\boldsymbol{\varphi}(\mathbf{X}, t)$ denote the invertible nonlinear deformation map which maps points $\mathbf{X} \in \mathfrak{B}_0$ of the reference configuration $\mathfrak{B}_0$ onto points $\mathbf{x} \in \mathfrak{B}$ of the current configuration $\mathfrak{B}$ at time $t \in \mathbb{R}_+$ via $\mathbf{x} = \boldsymbol{\varphi}(\mathbf{X}, t)$ with $\mathbf{X} = \boldsymbol{\varphi}^{-1}(\mathbf{x}, t)$. Then $\mathbf{F}$ defines the deformation gradient and J its Jacobian determinant with

$$\mathbf{F} = \mathbf{Grad}\, \boldsymbol{\varphi}(\mathbf{X}, t) \quad \text{and} \quad J := \det \mathbf{F} > 0, \tag{1}$$

where the latter is due to local impenetrability condition. The volume-preserving part of the deformation gradient is denoted by $\bar{\mathbf{F}}$ where

$$\bar{\mathbf{F}} := J^{-1/3}\mathbf{F} \quad \text{and} \quad \det \bar{\mathbf{F}} = 1. \tag{2}$$

[1] Throughout the paper, the following notation will be used. Assuming $\mathbf{a}$, $\mathbf{b}$, and $\mathbf{c}$ as three second-order tensors, together with Einstein's summation convention on repeated indices, $\mathbf{c} = \mathbf{a}\cdot\mathbf{b}$ represents the product with $c_{ik} = a_{ij}b_{jk}$. $d = \mathbf{a}:\mathbf{b} = a_{ij}b_{ij}$ represents the inner product where d is a scalar. $\mathbb{E} = \mathbf{a} \otimes \mathbf{b}$, $\mathbb{F} = \mathbf{a} \oplus \mathbf{b}$ and $\mathbb{G} = \mathbf{a} \ominus \mathbf{b}$ represent the tensor products with $E_{ijkl} = a_{ij}b_{kl}$, $F_{ijkl} = a_{ik}b_{jl}$ and $G_{ijkl} = a_{il}b_{jk}$, where $\mathbb{E}$, $\mathbb{F}$ and $\mathbb{G}$ represent fourth-order tensors. $\mathrm{dev}(\bullet) = [\bullet] - 1/3\ \mathrm{tr}(\bullet)\mathbf{1}$ and $\mathrm{tr}(\bullet)$ stand for the deviatoric part of and trace of $[\bullet]$, respectively, with $\mathbf{1}$ denoting the second-order identity tensor. $\mathrm{sym}(\bullet)$ and $\mathrm{skw}(\bullet)$ denote, respectively, symmetric and skew-symmetric parts of $[\bullet]$. $\dot{[\bullet]}$ gives the material time derivative of $[\bullet]$. $[\bullet]^{\mathrm{T}}$ and $[\bullet]^{-1}$ denote the transpose and the inverse of $[\bullet]$, respectively. Div $(\bullet)$ and div $(\bullet)$, respectively, designate the divergence operators with respect to the coordinates in the reference and current configurations. Analogously, **Grad** $(\bullet)$ and **grad** $(\bullet)$, respectively, designate the gradient operators with respect to the coordinates in the reference and current configurations. $\langle\bullet\rangle$ stands for the ramp function with $\langle\bullet\rangle = 1/2[\bullet + |\bullet|]$. $\log(\bullet)$ represents natural logarithm. Square brackets $[\ldots]$ are used to collect mathematical expressions, row-ordered vector components whereas round brackets $(\ldots)$ collect function arguments. Otherwise they, respectively, represent closed and open interval boundaries in a real space.

The right $\mathbf{C}$ and left $\mathbf{b}$ Cauchy–Green deformation tensors and their respective volume preserving counterparts $\overline{\mathbf{C}}$ and $\overline{\mathbf{b}}$ read

$$\mathbf{C}:=\mathbf{F}^{\mathrm{T}}\cdot\mathbf{F},\quad \overline{\mathbf{C}}:=\overline{\mathbf{F}}^{\mathrm{T}}\cdot\overline{\mathbf{F}}=J^{-2/3}\mathbf{C}\quad\text{with }\det\mathbf{C}=J^2\quad\text{and}\quad\det\overline{\mathbf{C}}=1, \tag{3}$$

$$\mathbf{b}:=\mathbf{F}\cdot\mathbf{F}^{\mathrm{T}},\quad \overline{\mathbf{b}}:=\overline{\mathbf{F}}\cdot\overline{\mathbf{F}}^{\mathrm{T}}=J^{-2/3}\mathbf{b}\quad\text{with }\det\mathbf{b}=J^2\quad\text{and}\quad\det\overline{\mathbf{b}}=1. \tag{4}$$

We use the following local multiplicative decomposition of the deformation gradient into elastic $\mathbf{F}^{\mathrm{e}}$ and viscoplastic $\mathbf{F}^{\mathrm{vp}}$ parts (Lee, 1969):

$$\mathbf{F}:=\mathbf{F}^{\mathrm{e}}\cdot\mathbf{F}^{\mathrm{vp}}\quad\text{with }J^{\mathrm{e}}:=\det\mathbf{F}^{\mathrm{e}}\equiv J\quad\text{and}\quad J^{\mathrm{vp}}:=\det\mathbf{F}^{\mathrm{vp}}=1 \tag{5}$$

which exploits plastic incompressibility. Hence, the volume preserving parts of elastic and plastic parts of the deformation gradient are defined, respectively, as

$$\overline{\mathbf{F}}^{\mathrm{e}}:=[J^{\mathrm{e}}]^{-1/3}\mathbf{F}^{\mathrm{e}}\quad\text{with }\overline{\mathbf{F}}^{\mathrm{vp}}:=[J^{\mathrm{vp}}]^{-1/3}\mathbf{F}^{\mathrm{vp}}\equiv\mathbf{F}^{\mathrm{vp}}. \tag{6}$$

The viscoplastic right Cauchy–Green deformation tensor $\mathbf{C}^{\mathrm{vp}}$ and elastic left Cauchy–Green deformation tensor $\mathbf{b}^{\mathrm{e}}$ read

$$\mathbf{C}^{\mathrm{vp}}:=[\mathbf{F}^{\mathrm{vp}}]^{\mathrm{T}}\cdot\mathbf{F}^{\mathrm{vp}}\equiv\mathbf{F}^{-1}\cdot\mathbf{b}^{\mathrm{e}}\cdot[\mathbf{F}]^{-\mathrm{T}}\quad\text{and}\quad\mathbf{b}^{\mathrm{e}}:=\mathbf{F}^{\mathrm{e}}\cdot[\mathbf{F}^{\mathrm{e}}]^{\mathrm{T}}. \tag{7}$$

The volume preserving counterparts $\overline{\mathbf{C}}^{\mathrm{vp}}$ and $\overline{\mathbf{b}}^{\mathrm{e}}$ can be given as

$$\overline{\mathbf{C}}^{\mathrm{vp}}:=\overline{\mathbf{F}}^{\mathrm{vp}^{\mathrm{T}}}\cdot\overline{\mathbf{F}}^{\mathrm{vp}}\equiv\mathbf{C}^{\mathrm{vp}}\quad\text{and}\quad\overline{\mathbf{b}}^{\mathrm{e}}:=\overline{\mathbf{F}}^{\mathrm{e}}\cdot\overline{\mathbf{F}}^{\mathrm{e}^{\mathrm{T}}}\equiv[J^{\mathrm{e}}]^{-2/3}\mathbf{b}^{\mathrm{e}}. \tag{8}$$

The spatial elastic logarithmic strains are denoted by $\boldsymbol{\epsilon}^{\mathrm{e}}$ with corresponding eigenvalues ϵ^{e}_A for $A=1,2,3$. Let b^{e}_A for $A=1,2,3$ denote the eigenvalues of $\mathbf{b}^{\mathrm{e}}$, the following connexions apply

$$\boldsymbol{\epsilon}^{\mathrm{e}}:=1/2\log\mathbf{b}^{\mathrm{e}}\quad\text{and}\quad\epsilon^{\mathrm{e}}_A:=\log\lambda^{\mathrm{e}}_A\quad\text{with }\lambda^{\mathrm{e}}_A:=\sqrt{b^{\mathrm{e}}_A}\quad\text{and}\quad\lambda^{\mathrm{e}}_1\lambda^{\mathrm{e}}_2\lambda^{\mathrm{e}}_3=J^{\mathrm{e}}, \tag{9}$$

$$\overline{\boldsymbol{\epsilon}}^{\mathrm{e}}:=1/2\log\overline{\mathbf{b}}^{\mathrm{e}}\quad\text{and}\quad\overline{\epsilon}^{\mathrm{e}}_A:=\log\overline{\lambda}^{\mathrm{e}}_A\quad\text{with }\overline{\lambda}^{\mathrm{e}}_A:=\sqrt{\overline{b}^{\mathrm{e}}_A}\quad\text{and}\quad\overline{\lambda}^{\mathrm{e}}_1\overline{\lambda}^{\mathrm{e}}_2\overline{\lambda}^{\mathrm{e}}_3=1. \tag{10}$$

Here, $\overline{\boldsymbol{\epsilon}}^{\mathrm{e}}$ denotes the volume preserving part of the spatial elastic logarithmic strains with corresponding eigenvalues $\overline{\epsilon}^{\mathrm{e}}_A$. Similarly, $\overline{b}^{\mathrm{e}}_A$ for $A=1,2,3$ denote the eigenvalues of $\overline{b}^{\mathrm{e}}$. λ^{e}_A for $A=1,2,3$ are referred to as elastic principal stretches, whereas $\overline{\lambda}^{\mathrm{e}}_A$ their isochoric counterparts. Note that since

$$\operatorname{tr}\boldsymbol{\epsilon}^{\mathrm{e}}=\log\lambda^{\mathrm{e}}_1+\log\lambda^{\mathrm{e}}_2+\log\lambda^{\mathrm{e}}_3=\log(\lambda^{\mathrm{e}}_1\lambda^{\mathrm{e}}_2\lambda^{\mathrm{e}}_3)=\log J^{\mathrm{e}}, \tag{11}$$

$\operatorname{tr}\boldsymbol{\epsilon}^{\mathrm{e}}$ and $\log J^{\mathrm{e}}$ can be used interchangeably. Finally, the following identity applies

$$\overline{\boldsymbol{\epsilon}}^{\mathrm{e}}\equiv\operatorname{dev}\boldsymbol{\epsilon}^{\mathrm{e}}=\boldsymbol{\epsilon}^{\mathrm{e}}-\tfrac{1}{3}\log J^{\mathrm{e}}\,\mathbf{1}. \tag{12}$$

2.2. Extension of the Thermodynamic Approach Represented in Simó and Miehe (1992)

Following the rational thermodynamics approach followed by Simó and Miehe (1992), the internal energy per unit reference volume is represented by $e(\mathbf{F}^{\mathrm{e}},\boldsymbol{\xi},\eta^{\mathrm{e}})$. The elastic entropy η^{e} is associated with the lattice and the vector $\boldsymbol{\xi}$ of strain-like internal variables responsible for irreversible mechanisms. For thermomechanical applications, an additively decoupled form of total entropy (per unit reference volume)

$$\eta=\eta^{\mathrm{e}}+\eta^{\mathrm{vpd}} \tag{13}$$

is claimed, utilizing its extensive property. η^{vpd} is the inelastic (configurational) entropy, associated with the dissipative mechanisms such as viscoplasticity, hardening and damage. Through the associative evolutionary forms emanating from conventional normality conditions together with a temperature dependent damage dissipation potential, one ends up with a natural additive split $\eta^{\mathrm{vpd}}=\eta^{\mathrm{vp}}+\eta^{\mathrm{d}}$. Hence, η^{vp} is linked to irreversible time dependent plastic structural changes, such as dislocation motion and lattice defects and η^{d} is linked to dissipative micro-structural changes accompanied by nucleation, growth and coalescence of micro-voids and micro-cracks. By this way, the framework given in Simó and Miehe (1992) is extended to account for damage induced effects.

In the current context, the vector of strain-like internal variables is defined as $\boldsymbol{\xi}=[\alpha,D]^{\mathrm{T}}$, with $\alpha\in\mathbb{R}_+$ and $D\in[0,1]$ being responsible for isotropic hardening and damage, respectively. Invariance requirements under arbitrary rigid body rotations on the intermediate configuration motivates the use of $e(\mathbf{F}^{\mathrm{e}},\boldsymbol{\xi},\eta^{\mathrm{e}})\mapsto e(\mathbf{b}^{\mathrm{e}},\boldsymbol{\xi},\eta^{\mathrm{e}})$. One may apply the Legendre transformation to derive

$$e(\mathbf{b}^{\mathrm{e}},\boldsymbol{\xi},\eta^{\mathrm{e}})=\Psi(\mathbf{b}^{\mathrm{e}},\boldsymbol{\xi},\Theta)+\Theta\eta^{\mathrm{e}}, \tag{14}$$

in which $\Psi(\mathbf{b}^{\mathrm{e}},\boldsymbol{\xi},\Theta)$ represents the Helmholtz free energy per unit reference volume, in terms of the absolute temperature $\Theta\in\mathbb{R}_+$ instead of elastic entropy. An additively decoupled form of $\Psi(\mathbf{b}^{\mathrm{e}},\boldsymbol{\xi},\Theta)$ reads

$$\Psi(\mathbf{b}^{\mathrm{e}}, \xi, \Theta) := \Psi^{\mathrm{e}}(\mathbf{b}^{\mathrm{e}}, D) + \Psi^{\Theta\mathrm{e}}(J^{\mathrm{e}}, \Theta, D) + \Psi^{\Theta}(\Theta) + \Psi^{\mathrm{vp}}(\alpha, \Theta), \tag{15}$$

where $\Psi^{\mathrm{e}}(\mathbf{b}^{\mathrm{e}}, D)$ denotes the damage affected pure elastic free energy which is stored by the body and can be recovered in a purely mechanical process.[2] Elastic structural entropy is constructed through the thermodilatational potential $\Psi^{\Theta\mathrm{e}}(J^{\mathrm{e}}, \Theta, D)$ which encapsulates the effect of damage on material's thermal expansion. $\Psi^{\Theta}(\Theta)$ is associated with the purely thermal entropy. $\Psi^{\mathrm{vp}}(\alpha, \Theta)$ stands for the viscoplastic free energy blocked in dislocations due to dislocation rearrangement. The relations between the nominal and the effective free energies follow

$$\Psi^{\mathrm{e}}(\mathbf{b}^{\mathrm{e}}, D) = [1 - D]\bar{\Psi}^{\mathrm{e}}(\mathbf{b}^{\mathrm{e}}) \quad \text{and} \quad \Psi^{\Theta\mathrm{e}}(J^{\mathrm{e}}, \Theta, D) = [1 - D]\bar{\Psi}^{\Theta\mathrm{e}}(J^{\mathrm{e}}, \Theta), \tag{16}$$

with $[\bar{\bullet}] := [\bullet]/[1 - D]$. Effective forms act on the intact material subscale, whereas nominal forms reflect the mathematically homogenized behavior under the influence of damage deterioration.

Equations of state: The second law of thermodynamics supplies the Clausius–Duhem inequality

$$0 \leq \Omega = \Omega_{\mathrm{conther}} + \Omega_{\mathrm{thermech}}, \tag{17}$$

where the respective dissipation expressions for the conductive thermal form and the local thermomechanical form per unit reference volume are denoted by $\Omega_{\mathrm{conther}}$ and $\Omega_{\mathrm{thermech}}$, with

$$\Omega_{\mathrm{conther}} := -\frac{1}{\Theta}\mathbf{q}\cdot\mathbf{grad}\,\Theta \quad \text{and} \quad \Omega_{\mathrm{thermech}} := \boldsymbol{\tau}:\mathbf{d} + \Theta\dot{\eta} - \dot{e}. \tag{18}$$

Here, $\mathbf{q}$ stands for the Kirchhoff-type heat flux, analogous with the Kirchhoff (weighted Cauchy) stress tensor $\boldsymbol{\tau}$ which is the work conjugate of the spatial rate of deformation tensor $\mathbf{d} := \mathrm{sym}(\mathbf{l})$ with $\mathbf{l} := \dot{\mathbf{F}}\cdot\mathbf{F}^{-1}$ denoting the spatial velocity gradient. Inequality (17) can be split into two more restrictive inequalities viz.

$$\Omega_{\mathrm{conther}} \geq 0 \quad \text{and} \quad \Omega_{\mathrm{thermech}} \geq 0. \tag{19}$$

In view of Eq. (18.1), satisfaction of $\Omega_{\mathrm{conther}} \geq 0$ merely depends upon an appropriately selected definition for $\mathbf{q}$. The latter inequality $\Omega_{\mathrm{thermech}} \geq 0$ requires more effort. Taking the material time derivative of the Legendre transform given in Eq. (14), $\dot{e} = \dot{\Psi} + \dot{\Theta}\eta^{\mathrm{e}} + \dot{\eta}^{\mathrm{e}}\Theta$, the latter inequality $\Omega_{\mathrm{thermech}} \geq 0$ can be represented as

$$0 \leq \Omega_{\mathrm{thermech}} = \boldsymbol{\tau}:\mathbf{d} + \Theta\dot{\eta}^{\mathrm{vpd}} - \dot{\Psi} - \dot{\Theta}\eta^{\mathrm{e}}, \tag{20}$$

where $\dot{\eta}^{\mathrm{vpd}} := \dot{\eta} - \dot{\eta}^{\mathrm{e}}$. Computation of $\dot{\Psi}$ requires the chain rule

$$\dot{\Psi} = \frac{\partial\Psi}{\partial\mathbf{b}^{\mathrm{e}}}:\dot{\mathbf{b}}^{\mathrm{e}} + \frac{\partial\Psi}{\partial\xi}\cdot\dot{\xi} + \frac{\partial\Psi}{\partial\Theta}\dot{\Theta}, \tag{21}$$

with

$$\dot{\mathbf{b}}^{\mathrm{e}} = \mathcal{L}_v\mathbf{b}^{\mathrm{e}} + \mathbf{l}\cdot\mathbf{b}^{\mathrm{e}} + \mathbf{b}^{\mathrm{e}}\cdot\left[\mathbf{l}\right]^{\mathrm{T}}. \tag{22}$$

Here, $\mathcal{L}_v(\bullet)$ stands for the objective Lie derivative of $(\bullet)$ via

$$\mathcal{L}_v\mathbf{b}^{\mathrm{e}} = \mathbf{F}\cdot\dot{\mathbf{G}}^{\mathrm{vp}}\cdot\left[\mathbf{F}\right]^{\mathrm{T}}, \tag{23}$$

in which $\mathbf{G}^{\mathrm{vp}} := [\mathbf{C}^{\mathrm{vp}}]^{-1}$ (Marsden and Hughes, 1994). Substituting Eqs. (21) and (22) into inequality (20) one finds

$$0 \leq \Omega_{\mathrm{thermech}} = \left[\boldsymbol{\tau} - 2\frac{\partial\Psi}{\partial\mathbf{b}^{\mathrm{e}}}\cdot\mathbf{b}^{\mathrm{e}}\right]:\mathbf{d} + 2\frac{\partial\Psi}{\partial\mathbf{b}^{\mathrm{e}}}\cdot\mathbf{b}^{\mathrm{e}}:\left[-\frac{1}{2}\mathcal{L}_v\mathbf{b}^{\mathrm{e}}\cdot\left[\mathbf{b}^{\mathrm{e}}\right]^{-1}\right] + \Theta\dot{\eta}^{\mathrm{vpd}} + \left[-\frac{\partial\Psi}{\partial\xi}\right]\cdot\dot{\xi} + \left[-\frac{\partial\Psi}{\partial\Theta} - \eta^{\mathrm{e}}\right]\dot{\Theta}. \tag{24}$$

Inelastic rates, i.e., $-1/2\,\mathcal{L}_v\mathbf{b}^{\mathrm{e}}\cdot[\mathbf{b}^{\mathrm{e}}]^{-1}$, $\dot{\eta}^{\mathrm{vpd}}$ and $\dot{\xi}$, tend to zero for any reversible process. Hence, following the arguments of Coleman and Gurtin (1967), for inequality (24) to be valid for arbitrary reversible changes in the observable variables $\mathbf{d}$ and $\dot{\Theta}$, the first and the last terms on the right-hand side must independently vanish to give[3]

$$\boldsymbol{\tau} = 2\frac{\partial\Psi}{\partial\mathbf{b}^{\mathrm{e}}}\cdot\mathbf{b}^{\mathrm{e}} = \frac{\partial\Psi}{\partial\epsilon^{\mathrm{e}}} \quad \text{and} \quad \eta^{\mathrm{e}} = -\frac{\partial\Psi}{\partial\Theta}. \tag{25}$$

Hence, elastic entropy is the conjugate variable of the temperature. Analogically, we devise

[2] To supply this form, for the sake of simplicity, we assume temperature independent elastic material parameters. For a treatment including temperature dependent elastic constants for thermoplasticity, see Čanadija and Brnić (2004).

[3] For Eq. (25.1), we use the chain rule of differentiation

$$\frac{\partial\Psi}{\partial\mathbf{b}^{\mathrm{e}}} = \frac{1}{2}\frac{\partial\Psi}{\partial\epsilon^{\mathrm{e}}}:\frac{\partial\log(\mathbf{b}^{\mathrm{e}})}{\partial\mathbf{b}^{\mathrm{e}}} \quad \text{and} \quad \left[\frac{\partial\Psi}{\partial\epsilon^{\mathrm{e}}}:\frac{\partial\log(\mathbf{b}^{\mathrm{e}})}{\partial\mathbf{b}^{\mathrm{e}}}\right]\cdot\mathbf{b}^{\mathrm{e}} = \frac{\partial\Psi}{\partial\epsilon^{\mathrm{e}}}.$$

See, e.g., de Souza Neto et al. (2008).

$$\boldsymbol{\varsigma} = -\frac{\partial \Psi}{\partial \boldsymbol{\xi}} \;\Rightarrow\; q = -\frac{\partial \Psi}{\partial \alpha} \quad \text{and} \quad Y^{\mathrm{d}} = -\frac{\partial \Psi}{\partial D}. \tag{26}$$

Here, $\boldsymbol{\varsigma}$ is the vector of stress-like internal variables which are dual to $\boldsymbol{\xi}$ with $\boldsymbol{\varsigma} = [q, Y^{\mathrm{d}}]^{\mathrm{T}}$. q is responsible for isotropic hardening in the form of yield locus expansion whereas Y^{d} is the thermodynamically formal damage conjugate variable. Additive decomposition of the potentials postulated in Eqs. (15) and (16) result in explicit representations for the state equations given in Eqs. (25):

$$\boldsymbol{\tau} = 2\big[1 - D\big]\left[\frac{\partial \tilde{\Psi}^{\mathrm{e}}}{\partial \boldsymbol{\epsilon}^{\mathrm{e}}} + \frac{\partial \tilde{\Psi}^{\Theta \mathrm{e}}}{\partial \boldsymbol{\epsilon}^{\mathrm{e}}}\right] \quad \text{and} \quad \eta^{\mathrm{e}} = -\,[1 - D]\frac{\partial \tilde{\Psi}^{\Theta \mathrm{e}}}{\partial \Theta} - \frac{\partial \Psi^{\Theta}}{\partial \Theta} - \frac{\partial \Psi^{\mathrm{vp}}}{\partial \Theta} \tag{27}$$

and in Eqs. (26)

$$q = -\frac{\partial \Psi^{\mathrm{vp}}}{\partial \alpha} \quad \text{and} \quad Y^{\mathrm{d}} = \tilde{\Psi}^{\mathrm{e}} + \tilde{\Psi}^{\Theta \mathrm{e}}. \tag{28}$$

Due to its dependence on $\tilde{\Psi}^{\Theta \mathrm{e}}$, the definition of the Kirchhoff stress tensor accounts for temperature dependent dilatational terms. Also, in this setting, the damage conjugate variable includes thermally motivated parts, as an extension of the conventional Lemaitre damage model. As a consequence of the temperature dependence of the viscoplastic free energy,[4] elastic entropy involves the term $\partial \Psi^{\mathrm{vp}}/\partial \Theta$.

Evolution equations: Substitution of Eqs. (25) and (26) back in inequality (24) with an explicit representation of the vectors $\boldsymbol{\xi}$ and $\boldsymbol{\varsigma}$ yields the following reduced dissipation inequality:

$$0 \le \Omega_{\mathrm{thermech}} = \boldsymbol{\tau} : \left[-\frac{1}{2}\mathcal{L}_v \mathbf{b}^{\mathrm{e}} \cdot \big[\mathbf{b}^{\mathrm{e}}\big]^{-1}\right] + q\,\dot{\alpha} + Y^{\mathrm{d}}\,\dot{D} + \Theta \dot{\eta}^{\mathrm{vpd}}. \tag{29}$$

The local thermomechanical dissipation $\Omega_{\mathrm{thermech}}$ can be split into thermal Ω_{ther} and mechanical Ω_{mech} parts (Coleman and Gurtin, 1967) to give

$$0 \le \Omega_{\mathrm{thermech}} := \Omega_{\mathrm{ther}} + \Omega_{\mathrm{mech}}, \tag{30}$$

where

$$\Omega_{\mathrm{ther}} := \Theta \dot{\eta}^{\mathrm{vpd}} \quad \text{and} \quad \Omega_{\mathrm{mech}} := \Omega^{\mathrm{vp}}_{\mathrm{mech}} + \Omega^{\mathrm{d}}_{\mathrm{mech}} \tag{31}$$

with

$$\Omega^{\mathrm{vp}}_{\mathrm{mech}} = \boldsymbol{\tau} : \left[-\frac{1}{2}\mathcal{L}_v \mathbf{b}^{\mathrm{e}} \cdot [\mathbf{b}^{\mathrm{e}}]^{-1}\right] + q\,\dot{\alpha} \quad \text{and} \quad \Omega^{\mathrm{d}}_{\mathrm{mech}} = Y^{\mathrm{d}}\,\dot{D}. \tag{32}$$

Similar to what is done for inequality (19) we can split inequality (31) into two stronger inequalities

$$\Omega_{\mathrm{ther}} \ge 0 \quad \text{and} \quad \Omega_{\mathrm{mech}} \ge 0. \tag{33}$$

The evolutionary forms exploit the hypothesis of generalized standard materials, which proposes the existence of normality rules (Maugin, 1992). Accordingly, a loading function Φ additively decoupled into a temperature dependent viscoplastic potential Φ^{vp} and a temperature dependent damage dissipation potential Φ^{d} is postulated:

$$\Phi(\boldsymbol{\tau}, q, Y^{\mathrm{d}}, \Theta, D) := \Phi^{\mathrm{vp}}(\bar{\boldsymbol{\tau}}, q, \Theta) + \Phi^{\mathrm{d}}(Y^{\mathrm{d}}, \Theta, D). \tag{34}$$

Owing to the fact that viscoplastic flow is physically possible at the undamaged material sub-scale, the formulation of Φ^{vp} takes place in the effective Kirchhoff stress space. Extending the standard normality rule and using Eq. (34) the flow rule is computed viz.

$$-\frac{1}{2}\mathcal{L}_v \mathbf{b}^{\mathrm{e}} \cdot \big[\mathbf{b}^{\mathrm{e}}\big]^{-1} = \dot{\gamma}\frac{\partial \Phi}{\partial \boldsymbol{\tau}} \quad \Rightarrow \quad \mathcal{L}_v \mathbf{b}^{\mathrm{e}} = -\,2\frac{\dot{\gamma}}{1 - D}\frac{\partial \Phi^{\mathrm{vp}}}{\partial \bar{\boldsymbol{\tau}}} \cdot \mathbf{b}^{\mathrm{e}}, \tag{35}$$

which is coaxial with the Kirchhoff stress due to isotropy. Here, $\dot{\gamma}$ represents the viscoplastic multiplier. The current approach generalizes the viscoplasticity of overstress-type[5] by considering all processes to be viscoplastic for stress states outside the thermoelastic domain, i.e., $\Phi^{\mathrm{vp}} > 0$. Thermoelastic domain, on the other hand, is represented by $\Phi^{\mathrm{vp}} < 0$. Accordingly, in spirit of Perzyna we postulate[6]

[4] In the work of Simó and Miehe (1992) this kind of a coupling at the free energy level is bypassed in the theory, however, used in the application problems.

[5] Viscosity has also a regularizing effect on the mesh dependence of the softening response. In context of damage-coupled plasticity, using Perzyna-type rate dependence, single surface overstress-type viscous forms are utilized by Reckwerth and Tsakmakis (2003) and Simone (2003) among others.

[6] On the contrary, rate independent theories do not allow the condition $\Phi^{p} > 0$. Thus, the definition of the plastic multiplier $\dot{\gamma}^{\mathrm{p}}$ relies on the Kuhn–Tucker optimality conditions

$$\dot{\gamma} := \begin{cases} 0 & \Phi^{\mathrm{vp}} \le 0, \\ \dfrac{1}{t_\star} f(\Phi^{\mathrm{vp}}) & \Phi^{\mathrm{vp}} > 0, \end{cases} \tag{36}$$

where $t_\star$ is the characteristic relaxation time and the nondimensional function f is a monotonically increasing function of Φ^{vp} and it is required that $f(\Phi^{\mathrm{vp}}) = 0$ for $\Phi^{\mathrm{vp}} = 0$. As $t_\star \to 0$ rate independent plasticity is recovered whereas $t_\star \to \infty$ represents the elastic theory since all inelastic processes cease to evolve. Also for zero elastic limit creep is carried out. Having $\dot{\gamma}$ defined, the rates of the scalar internal variables α, D and η^{vpd} read

$$\dot{\alpha} = \dot{\gamma}\frac{\partial \Phi}{\partial q}, \quad \dot{D} = \dot{\gamma}\frac{\partial \Phi}{\partial Y^{\mathrm{d}}} \quad \text{and} \quad \dot{\eta}^{\mathrm{vpd}} = \dot{\gamma}\frac{\partial \Phi}{\partial \Theta}. \tag{37}$$

In view of Eq. (34), Eq. (37) can be reiterated as

$$\dot{\alpha} = \dot{\gamma}\frac{\partial \Phi^{\mathrm{vp}}}{\partial q}, \quad \dot{D} = \dot{\gamma}\frac{\partial \Phi^{\mathrm{d}}}{\partial Y^{\mathrm{d}}} \quad \text{and} \quad \dot{\eta}^{\mathrm{vpd}} = \dot{\gamma}\frac{\partial \Phi^{\mathrm{vp}}}{\partial \Theta} + \dot{\gamma}\frac{\partial \Phi^{\mathrm{d}}}{\partial \Theta}. \tag{38}$$

In context of the maximum inelastic dissipation postulate, multi-surface damage-plasticity models which account for separate viscoplastic and damage multipliers (in the form of Lagrange multipliers), damage evolution in the absence of plastic flow is possible, Hansen and Schreyer (1994). In the current formulation, on the other hand, damage concurrently occurs with viscoplasticity since the growths of both α and D depend on the viscoplastic multiplier $\dot{\gamma}$ as the consequence of kinematic coupling between plasticity and damage. Such an application has proven convenient in ductile metal damage, where the dislocation pile-ups supply as a void nucleation source. This also postulates that the evolution of the inelastic entropy depends on both the viscoplasticity and the damage dissipation potentials, which is an extension to Simó and Miehe (1992) where no damage mechanism is taken into account. One may represent the inelastic entropy production given in Eq. (38.3) in an additive form in terms of viscoplastic and damage parts

$$\dot{\eta}^{\mathrm{vpd}} = \dot{\eta}^{\mathrm{vp}} + \dot{\eta}^{\mathrm{d}} \quad \text{with} \quad \dot{\eta}^{\mathrm{vp}} = \dot{\gamma}\frac{\partial \Phi^{\mathrm{vp}}}{\partial \Theta} \quad \text{and} \quad \dot{\eta}^{\mathrm{d}} = \dot{\gamma}\frac{\partial \Phi^{\mathrm{d}}}{\partial \Theta}. \tag{39}$$

Finally, for the temperature evolution equation, following Simó and Miehe (1992), we start with local energy balance equation, i.e., the first law of thermodynamics

$$-J\,\mathrm{div}\left(\frac{\mathbf{q}}{J}\right) + R = \dot{e} - \boldsymbol{\tau}\colon \mathbf{d}. \tag{40}$$

Here, R represents the heat source. In the first term on the left-hand side, $\mathbf{q}/J$ represents conversion of the heat flux from Kirchhoff to Cauchy-type whereas the factor J in front of $\mathrm{div}(\frac{\mathbf{q}}{J})$ guarantees that the quantity is computed per unit reference volume. Using Eqs. (13), (20), (30) and (31.2) and the material time derivative of Eq. (25.2) one carries out

$$\dot{e} - \boldsymbol{\tau}\colon \mathbf{d} = -\Omega_{\mathrm{mech}} + \Theta\left[\dot{\eta} - \dot{\eta}^{\mathrm{vpd}}\right] = -\Omega_{\mathrm{mech}} + \mathcal{H} + \dot{\Theta} c, \tag{41}$$

where $\mathcal{H}$ denotes the elastic-plastic-damage structural heating which is related to the latent elastic and inelastic structural changes and c denotes the heat capacity with

$$\mathcal{H} := -\Theta\frac{\partial\left(\boldsymbol{\tau}\colon \mathbf{d} - \Omega_{\mathrm{mech}}\right)}{\partial \Theta} \quad \text{and} \quad c := -\Theta\frac{\partial^2 \Psi}{\partial \Theta^2}. \tag{42}$$

Substituting Eq. (41) into the right-hand side of Eq. (40) and rearranging, one reaches the temperature evolution equation

$$c\dot{\Theta} = \Omega_{\mathrm{mech}} - \mathcal{H} - J\,\mathrm{div}\left(\frac{\mathbf{q}}{J}\right) + R. \tag{43}$$

Note that Eq. (43) is in agreement with Simó and Miehe (1992). However, in the current context, Ω_{mech} inherently involves damage effects. Moreover, $\mathcal{H}$ is found as

$$\mathcal{H} = -\Theta\left[\frac{\partial}{\partial \Theta}\left(\frac{\partial \Psi}{\partial \mathbf{b}^{\mathrm{e}}}\right)\colon \dot{\mathbf{b}}^{\mathrm{e}} + \frac{\partial}{\partial \Theta}\left(\frac{\partial \Psi}{\partial \alpha}\right)\dot{\alpha} + \frac{\partial}{\partial \Theta}\left(\frac{\partial \Psi}{\partial D}\right)\dot{D}\right]. \tag{44}$$

(*footnote continued*)

$$\dot{\gamma}^{\mathrm{p}} \ge 0, \quad \Phi^{p}(\tilde{\boldsymbol{\tau}}, q, \Theta) \le 0 \quad \text{and} \quad \dot{\gamma}^{\mathrm{p}}\Phi^{p}(\tilde{\boldsymbol{\tau}}, q, \Theta) = 0.$$

3. Specification of constitutive functions for metals

In this section the potentials are specified in order to derive the explicit representations of state laws and evolutionary equations. For elasticity, one may postulate a volumetric-isochoric split for the effective elastic potential,

$$\tilde{\Psi}^{\mathrm{e}}(\mathbf{b}^{\mathrm{e}}) = \tilde{\Psi}^{\mathrm{e}}_{\mathrm{vol}}(J^{\mathrm{e}}) + \tilde{\Psi}^{\mathrm{e}}_{\mathrm{iso}}(\bar{\epsilon}^{\mathrm{e}}), \tag{45}$$

where $\tilde{\Psi}^{\mathrm{e}}_{\mathrm{vol}}$ represents the volumetric part and $\tilde{\Psi}^{\mathrm{e}}_{\mathrm{iso}}$ the isochoric part. With the use of the principals of the tensor arguments in representation of the isotropic tensor functions we have $\tilde{\Psi}^{\mathrm{e}}_{\mathrm{iso}}(\bar{\epsilon}^{\mathrm{e}}) \mapsto \tilde{\Psi}^{\mathrm{e}}_{\mathrm{iso}}(\bar{\epsilon}^{\mathrm{e}}_A)$ for $A = 1, 2, 3$, and

$$\tilde{\Psi}^{\mathrm{e}}_{\mathrm{vol}}(J^{\mathrm{e}}) := \frac{1}{2} H \log^2\left(J^{\mathrm{e}}\right) \quad \text{and} \quad \tilde{\Psi}^{\mathrm{e}}_{\mathrm{iso}}(\bar{\epsilon}^{\mathrm{e}}_A) := \mu\left[\bar{\epsilon}^{\mathrm{e}2}_1 + \bar{\epsilon}^{\mathrm{e}2}_2 + \bar{\epsilon}^{\mathrm{e}2}_3\right]. \tag{46}$$

Here, H and μ denote the bulk and the shear modulus, respectively.[7] Denoting the linear coefficient of thermal expansion by α_Θ and the reference temperature by Θ_0 volumetric elastic deformation is associated with the thermal effects through the following effective thermodilatational potential (see, e.g., Hakansson et al., 2006):

$$\tilde{\Psi}^{\Theta\mathrm{e}}(J^{\mathrm{e}}, \Theta) := -3\, H\, \alpha_\Theta [\Theta - \Theta_0] \log\left(J^{\mathrm{e}}\right). \tag{47}$$

For the plastic part, the following isotropic hardening potential is common which is associated with a combined linear and saturation-type. In the presence of thermal coupling, this potential depends on temperature and reads

$$\Psi^{\mathrm{vp}}(\alpha, \Theta) := \frac{1}{2} K(\Theta)\alpha^2 + [\tau_{y\infty}(\Theta) - \tau_{y0}(\Theta)]\left[\alpha - \frac{1 - \exp(-\delta\alpha)}{\delta}\right]. \tag{48}$$

Here, $K(\Theta)$ represents the temperature dependent linear hardening coefficient. τ_{y0} and $\tau_{y\infty}$ denote the initial and the saturation yield stress, respectively. δ is the hardening saturation exponent. One has $\Psi^{\mathrm{vp}}(\alpha, \Theta) \to 0$ for $\alpha \to 0$, as required. Defining functions $g_{\omega^{\mathrm{vp}}}(\Theta)$ and $g_{\omega^{\mathrm{d}}}(\Theta)$ as

$$g_{\omega^{\mathrm{vp}}}(\Theta) := 1 - [\Lambda(\Theta)]^{\omega^{\mathrm{vp}}} \quad \text{and} \quad g_{\omega^{\mathrm{d}}}(\Theta) := 1 - [\Lambda(\Theta)]^{\omega^{\mathrm{d}}}, \tag{49}$$

where ω^{vp} and ω^{d} denote the viscoplastic and damage thermal softening exponents, respectively, and $\Lambda(\Theta)$ represents the homologous temperature with

$$\Lambda(\Theta) = \frac{\Theta - \Theta_0}{\Theta_{\mathrm{melt}} - \Theta_0}, \tag{50}$$

where Θ_{melt} denotes the melting temperature, and using the notation $K_0 = K(\Theta_0)$, $\tau_{y0,0} = \tau_{y0}(\Theta_0)$ and $\tau_{y\infty,0} = \tau_{y\infty}(\Theta_0)$ we adopt nonlinear thermoplasticity viz.

$$K(\Theta) := g_{\omega^{\mathrm{vp}}}(\Theta) K_0, \quad \tau_{y0}(\Theta) := g_{\omega^{\mathrm{vp}}}(\Theta)\tau_{y0,0} \quad \text{and} \quad \tau_{y\infty}(\Theta) := g_{\omega^{\mathrm{vp}}}(\Theta)\tau_{y\infty,0}. \tag{51}$$

Finally, letting $-c_0 = \Theta \partial^2 \tilde{\Psi}^{\Theta} / \partial\Theta^2$ denote the temperature-independent heat capacity of the material at constant deformation, we postulate the following pure thermal potential:

$$\Psi^{\Theta}(\Theta) := c_0\left[\left[\Theta - \Theta_0\right] - \Theta \log\left(\frac{\Theta}{\Theta_0}\right)\right], \tag{52}$$

Hence, using Eq. (45) with Eqs. (46)–(48) along with Eq. (42.2), heat capacity c reads

$$c = c_0 - \Theta g''_{\omega^{\mathrm{vp}}} \Psi^{\mathrm{vp}}(\alpha, \Theta_0), \tag{53}$$

where $g''_{\omega^{\mathrm{vp}}} = \partial^2 g_{\omega^{\mathrm{vp}}} / \partial\Theta^2$. Note that selecting $\omega^{\mathrm{vp}} = 1$, i.e., linear temperature dependence of the isotropic hardening potential, Eq. (53) reduces to $c \to c_0$ with $g''_{\omega^{\mathrm{vp}}} \Psi^{\mathrm{vp}} \to 0$.

The total Kirchhoff stress tensor can be decomposed additively into volumetric $p\mathbf{1}$ and deviatoric $\mathbf{s}$ parts to give $\boldsymbol{\tau} = p\mathbf{1} + \mathbf{s}$ where $p := 1/3\ \mathrm{tr}\,\boldsymbol{\tau}$ represents the mean stress and $\mathbf{s} := \mathrm{dev}\,\boldsymbol{\tau}$. Using the connexions $\tilde{p} = p/[1 - D]$, $\tilde{\mathbf{s}} = \mathbf{s}/[1 - D]$ and $\tilde{\boldsymbol{\tau}} = \boldsymbol{\tau}/[1 - D]$ this amounts for $\tilde{\boldsymbol{\tau}} = \tilde{p}\mathbf{1} + \tilde{\mathbf{s}}$ where $\tilde{p}$ and $\tilde{\mathbf{s}}$ represent *effective* mean (Kirchhoff) stress and the deviatoric stress tensor, respectively. Substituting Eqs. (45) with (46) and (47) into Eq. (25.1) and noting that $\partial J^{\mathrm{e}} / \partial \boldsymbol{\epsilon}^{\mathrm{e}} = \mathbf{1}$, $\tilde{p}$ and $\tilde{\mathbf{s}}$ are computed as[8]

[7] This quadratic form in terms of Hencky measure of elastic strains preserves validity for a large class of materials up to moderately large deformations (Weber and Anand, 1990), but does not satisfy the polyconvexity condition (Lin et al., 2006).

[8] Thanks to elastic isotropy, $\boldsymbol{\epsilon}^{\mathrm{e}}$ and $\tilde{\boldsymbol{s}}$ are coaxial, and, thus share identical eigenbases: $\mathbf{m}^A = \boldsymbol{\nu}^A \otimes \boldsymbol{\nu}^A$, where $\boldsymbol{\nu}^A$ represents the corresponding eigenvectors with $A = 1, 2, 3$.

$$\tilde{p} = H\,\log(J^{\mathrm{e}}) - 3\,H\,\alpha_{\varTheta}[\varTheta - \varTheta_0] \quad \text{and} \quad \tilde{\mathbf{s}} = 2\mu\,\bar{\boldsymbol{\varepsilon}}^{\mathrm{e}}. \tag{54}$$

Using Eqs. (28) along with Eqs. (45)–(48) gives the plastic isotropic hardening function q with temperature effects

$$q(\alpha,\,\varTheta) = g_{\omega^{\mathrm{vp}}}(\varTheta)q(\alpha,\,\varTheta_0) \quad \text{where } q(\alpha,\,\varTheta_0) = -\,K_0\,\alpha - \Big[\,\tau_{y\infty,0} - \tau_{y0,0}\Big]\Big[\,1 - \exp(\,-\,\delta\alpha)\Big] \tag{55}$$

and the damage conjugate variable Y^{d} associated with the temperature dependent total thermoelastic energy release rate

$$Y^{\mathrm{d}} = \tfrac{1}{2}H\Big[\log\big(J^{\mathrm{e}}\big)\Big]^2 + \mu\Big[\,\bar{\epsilon}_1^{\mathrm{e}2} + \bar{\epsilon}_2^{\mathrm{e}2} + \bar{\epsilon}_3^{\mathrm{e}2}\Big] - 3\,H\,\alpha_{\varTheta}[\varTheta - \varTheta_0]\log\big(J^{\mathrm{e}}\big). \tag{56}$$

Finally, in view of Eq. (25.2) together with Eqs. (47) and (48) one derives the following expression for η^{e}:

$$\eta^{\mathrm{e}} = \big[\,1 - D\big]3\,H\,\alpha_{\varTheta}\log\big(J^{\mathrm{e}}\big) + c_0\,\log\left(\frac{\varTheta}{\varTheta_0}\right) - g'_{\omega^{\mathrm{vp}}}(\varTheta)\left[\frac{1}{2}K_0\,\alpha^2 + [\tau_{y\infty,0} - \tau_{y0,0}]\left[\,\delta + \frac{\exp(\,-\,\delta\alpha)}{\delta}\right]\right]. \tag{57}$$

where using Eqs. (49), $g'_{\omega^{\mathrm{vp}}}(\varTheta) = dg_{\omega^{\mathrm{vp}}}(\varTheta)/d\varTheta$ and $g'_{\omega^{\mathrm{d}}}(\varTheta) = dg_{\omega^{\mathrm{d}}}(\varTheta)/d\varTheta$ one has

$$g'_{\omega^{\mathrm{vp}}}(\varTheta) = -\,\frac{\omega^{\mathrm{vp}}}{\varTheta_{\mathrm{melt}} - \varTheta_0}\varLambda(\varTheta)^{\omega^{\mathrm{vp}}-1} \quad \text{and} \quad g'_{\omega^{\mathrm{d}}}(\varTheta) = -\,\frac{\omega^{\mathrm{d}}}{\varTheta_{\mathrm{melt}} - \varTheta_0}\varLambda(\varTheta)^{\omega^{\mathrm{d}}-1}. \tag{58}$$

Plastic incompressibility allows to represent the yield function $\varPhi^{\mathrm{vp}}$ in terms of the stress deviator, i.e., $\varPhi^{\mathrm{vp}}(\tilde{\boldsymbol{\tau}},\,q;\,\varTheta)\mapsto\varPhi^{\mathrm{vp}}(\tilde{\mathbf{s}},\,q;\,\varTheta)$. Plastic isotropy, on the other hand, concedes a representation in terms of effective deviatoric stress principals $\tilde{s}_A$ for $A = 1, 2, 3$ through $\varPhi^{\mathrm{vp}}(\tilde{\mathbf{s}},\,q;\,\varTheta)\mapsto\varPhi^{\mathrm{vp}}(\tilde{s}_A,\,q;\,\varTheta)$ as in the case of Eq. (46.2). Hence, using a J_2 theory for plasticity together with a four-parameter damage dissipation potential (see, e.g., Lemaitre, 1996), we have:

$$\varPhi^{\mathrm{vp}}(\tilde{s}_A,\,q,\,\varTheta) := \Big[\,\tilde{s}_1^2 + \tilde{s}_2^2 + \tilde{s}_3^2\Big]^{1/2} - \sqrt{\frac{2}{3}}y(q,\,\varTheta), \tag{59}$$

$$\varPhi^{\mathrm{d}}(Y^{\mathrm{d}},\,\varTheta,\,D) := \frac{1}{s+1}\frac{a(\varTheta)}{[1-D]^r}\left[\frac{\langle Y^{\mathrm{d}} - Y_0^{\mathrm{d}}\rangle}{a(\varTheta)}\right]^{s+1}. \tag{60}$$

Here, $y(q,\,\varTheta) = [\tau_{y0}(\varTheta) - q(\alpha,\,\varTheta)]$ represents the hardening/softening function with thermal coupling. In fact, $[\tilde{s}_1^2 + \tilde{s}_2^2 + \tilde{s}_3^2]^{1/2}$ corresponds to a norm of $\tilde{\mathbf{s}}$ via $\|\tilde{\mathbf{s}}\| := [\tilde{s}_1^2 + \tilde{s}_2^2 + \tilde{s}_3^2]^{1/2}$. Y_0^{d} represents the threshold for Y^{d} below which damage ceases to evolve. r, s and $a(\varTheta)$ represent other damage related material parameters. Using Eq. (49.2) with $a_0 = a(\varTheta_0)$ a nonlinear temperature dependence is chosen for the damage parameter $a(\varTheta)$ via

$$a(\varTheta) = g_{\omega^{\mathrm{d}}}(\varTheta)a_0. \tag{61}$$

The choice of $f(\varPhi^{\mathrm{vp}})$ is defined using a Norton-type formulation viz.

$$f(\varPhi^{\mathrm{vp}}) := \left[\frac{\varPhi^{\mathrm{vp}}(\tilde{s}_A,\,q,\,\varTheta)}{\kappa^{\mathrm{vp}}}\right]^{1/m}, \tag{62}$$

where κ^{vp} is the constant drag stress and m the viscoplastic exponent. In view of Eq. (62), Eq. (36) can be rewritten as

$$\dot{\gamma} = \frac{1}{t_\star}\left\langle\frac{\varPhi^{\mathrm{vp}}(\tilde{s}_A,\,q,\,\varTheta)}{\kappa^{\mathrm{vp}}}\right\rangle^{1/m}. \tag{63}$$

Exploiting the condition $n_A := s_A/\|\mathbf{s}\| \equiv \partial\varPhi^{\mathrm{vp}}/\partial\tilde{\tau}_A \equiv \tilde{s}_A/\|\tilde{\mathbf{s}}\| =: \tilde{n}_A$ as well as the fact that the eigenbases for the nominal and effective stresses are equivalent, i.e., $\boldsymbol{\nu}^A \otimes \boldsymbol{\nu}^A \equiv \tilde{\boldsymbol{\nu}}^A \otimes \tilde{\boldsymbol{\nu}}^A$, and using Eq. (35.2) with Eq. (59), the viscoplastic flow rule is derived as

$$\frac{\partial\varPhi^{\mathrm{vp}}}{\partial\tilde{\boldsymbol{\tau}}} = \sum_{A=1}^{3} n_A\,\boldsymbol{\nu}^A \otimes \boldsymbol{\nu}^A \;\Rightarrow\; \mathcal{L}_v\mathbf{b}^{\mathrm{e}} = -\,2\frac{\dot{\gamma}}{1-D}\left[\sum_{A=1}^{3} n_A\,\boldsymbol{\nu}^A \otimes \boldsymbol{\nu}^A\right]\cdot\mathbf{b}^{\mathrm{e}} \tag{64}$$

Coming to the kinetic relations for the scalar strain-like variables α and D, using Eqs. (37) along with Eqs. (59) and (60) gives

$$\frac{\partial\varPhi^{\mathrm{vp}}}{\partial q} = \sqrt{\frac{2}{3}} \quad \Rightarrow \quad \dot{\alpha} = \dot{\gamma}\sqrt{\frac{2}{3}}, \tag{65}$$

$$\frac{\partial\varPhi^{\mathrm{d}}}{\partial Y^{\mathrm{d}}} = \frac{1}{[1-D]^r}\left[\frac{\langle Y^{\mathrm{d}} - Y_0^{\mathrm{d}}\rangle}{a(\varTheta)}\right]^s \quad \Rightarrow \quad \dot{D} = \dot{\gamma}\frac{1}{[1-D]^r}\left[\frac{\langle Y^{\mathrm{d}} - Y_0^{\mathrm{d}}\rangle}{a(\varTheta)}\right]^s. \tag{66}$$

Using Eq. (32.1) with Eq. (65), $\Omega^{\mathrm{vp}}_{\mathrm{mech}}$ yields

$$\Omega^{\mathrm{vp}}_{\mathrm{mech}} = \dot{\gamma}\left[\|\tilde{\mathbf{s}}\| + \sqrt{\frac{2}{3}}q(\alpha, \Theta)\right]. \tag{67}$$

Note that at the rate independent limit one has $\Omega^{\mathrm{vp}}_{\mathrm{mech}} = \dot{\gamma}\sqrt{2/3}\,\tau_{y0}(\Theta)$ with $\dot{\gamma}\Phi^{\mathrm{vp}} = 0$, in agreement with Simó and Miehe (1992). The details of this derivation are found in Appendix D. Via Eqs. (32.2) and (66) damage dissipation reads

$$\Omega^{\mathrm{d}}_{\mathrm{mech}} = \dot{\gamma}\frac{Y^{\mathrm{d}}}{[1-D]^r}\left[\frac{\langle Y^{\mathrm{d}} - Y^{\mathrm{d}}_0\rangle}{a(\Theta)}\right]^s. \tag{68}$$

Using Eq. (31.1) along with Eqs. (67) and (68) the total mechanical dissipation Ω_{mech} is derived as[9]

$$\Omega_{\mathrm{mech}} = \dot{\gamma}\left[\|\tilde{\mathbf{s}}\| + \sqrt{\frac{2}{3}}q(\alpha, \Theta) + \frac{Y^{\mathrm{d}}}{[1-D]^r}\left[\frac{\langle Y^{\mathrm{d}} - Y^{\mathrm{d}}_0\rangle}{a(\Theta)}\right]^s\right]. \tag{69}$$

This expression is of crucial importance in the current thermoinelastic framework. Besides constituting the heat source, it also accounts for the term that is used in linearization of the weak form of the thermal problem.

Using Eq. (39.2) the growth of the viscoplastic entropy is derived using $\dot{\eta}^{\mathrm{vp}} = \partial\Phi^{\mathrm{vp}}/\partial\Theta$ at constant $\tilde{s}_A$ for $A = 1, 2, 3$ and q as

$$\dot{\eta}^{\mathrm{vp}} = -\dot{\gamma}\sqrt{\frac{2}{3}}g'_{\omega^{\mathrm{vp}}}(\Theta)\tau_{y0,0}. \tag{70}$$

For the growth of the inelastic entropy associated with damage we revert to Eq. (39.3) and use $\dot{\eta}^{\mathrm{d}} = \partial\Phi^{\mathrm{d}}/\partial\Theta$ at constant D and Y to give

$$\dot{\eta}^{\mathrm{d}} = -\dot{\gamma}g'_{\omega^{\mathrm{d}}}(\Theta)a_0\frac{s}{s+1}\frac{1}{[1-D]^r}\left[\frac{\langle Y^{\mathrm{d}} - Y^{\mathrm{d}}_0\rangle}{a(\Theta)}\right]^{s+1}. \tag{71}$$

The second law of thermodynamics as given in Eq. (33.2) places the restriction $\dot{\eta}^{\mathrm{vpd}} \geq 0$. Since the expressions in Eqs. (70) and (71) add up to the rate of total inelastic entropy production $\dot{\eta}^{\mathrm{vpd}}$ with Eq. (39.1), one may suggest two stronger inequalities, such as $\dot{\eta}^{\mathrm{vp}} \geq 0$ and $\dot{\eta}^{\mathrm{d}} \geq 0$. The former is naturally satisfied, where in view of Eqs. (51) and (50) thermal softening of the yield stress is addressed. This condition, also named as the yield locus contraction with temperature, reflects the experimental evidences. The latter inequality, however, may put an overrestriction on the material parameters.

Finally, coming to the time sensitive thermal dissipation analysis an isotropic Eulerian Fourier law for the *effective* Kirchhoff heat flux is assumed viz. (Miehe, 1995)

$$\tilde{\mathbf{q}} = -k\,\mathbf{grad}\,\Theta, \tag{72}$$

where $k > 0$ is the isotropic heat conduction coefficient in the absence of damage effects. The *homogenized* flux in the interior of the body is assumed to read (Ganczarski, 2003)

$$\mathbf{q} = [1-D]\tilde{\mathbf{q}}. \tag{73}$$

With Eq. (73), the negative effect of damage on the ability of the body to transfer thermal energy from one point to another in the presence of temperature gradients is reflected via the factor $[1-D]$. For a completely damaged material point (if $D \to 1$ one has $[1-D]k \to 0$) no heat conduction takes place. Substituting Eqs. (73) in the conductive thermal dissipation inequality given in Eq. (18.1) yields

$$\Omega_{\mathrm{conther}} = \big[1-D\big]\frac{1}{\Theta}k\,\mathbf{grad}\,\Theta\cdot\mathbf{grad}\,\Theta \geq \mathbf{0} \tag{74}$$

as required.[10]

[9] Since, in general, $\Omega^{\mathrm{d}}_{\mathrm{mech}} \ll \Omega^{\mathrm{vp}}_{\mathrm{mech}}$ it may be advocated that $\Omega_{\mathrm{mech}} \simeq \Omega^{\mathrm{vp}}_{\mathrm{mech}}$.

[10] Note that the expression for $\mathbf{q}$ can also be derived from the damage affected version of the so-called Fourier dissipation potential Υ postulated per unit reference volume as

$$\Upsilon(\mathbf{grad}\,\Theta, D) = \big[1-D\big]\tilde{\Upsilon}(\mathbf{grad}\,\Theta) \quad \text{and} \quad \tilde{\Upsilon}(\mathbf{grad}\,\Theta) = -\tfrac{1}{2}k\,\mathbf{grad}\,\Theta\cdot\mathbf{grad}\,\Theta,$$

with $\mathbf{q} = \partial\Upsilon/\partial[\mathbf{grad}\,\Theta]$.

Box 1–A summary of the proposed model for general 3D stress-state.

(i) Multiplicative kinematics:

$\mathbf{F} = \mathbf{F}^{\mathrm{e}}\cdot\mathbf{F}^{\mathrm{vp}}$.

(ii) Thermoelastic stress–strain relationship:

$\boldsymbol{\tau} = [1 - D][\tilde{p}\mathbf{1} + \tilde{\mathbf{s}}]$,

where

$\tilde{p} = H\log(J^{e}) - 3H\,\alpha_{\varTheta}[\varTheta - \varTheta_0]$ and $\tilde{\mathbf{s}} = 2\mu\,\bar{\boldsymbol{\varepsilon}}^{\mathrm{e}}$.

(iii) State laws for hardening and damage conjugate variables:

$q = -g_{\omega^{\mathrm{vp}}}(\varTheta)\Big[K_0\,\alpha + \Big[\tau_{y\infty,0} - \tau_{y0,0}\Big]\Big[1 - \exp(-\delta\alpha)\Big]\Big]$,
$Y^{\mathrm{d}} = \frac{1}{2}H\Big[\log\big(J^{\mathrm{e}}\big)\Big]^2 + \mu\Big[\bar{\varepsilon}_1^{\mathrm{e}2} + \bar{\varepsilon}_2^{\mathrm{e}2} + \bar{\varepsilon}_3^{\mathrm{e}2}\Big] - 3\,H\,\alpha_{\varTheta}[\varTheta - \varTheta_0]\log\big(J^{\mathrm{e}}\big)$.

(iv) Thermoelastic domain in (principal) stress space (single surface):

$\mathbb{E}_{\tau} = \{[\tilde{s}_A, q, \varTheta] \in \mathbb{R}^3 \times \mathbb{R}_- \times \mathbb{R}_+ : \varPhi^{\mathrm{vp}}(\tilde{s}_A, q, \varTheta) \le 0\}$,

where $A = 1, 2, 3$ and using $y(q, \varTheta) = \tau_{y0}(\varTheta) - q$

$\varPhi^{\mathrm{vp}}(\tilde{s}_A, q, \varTheta) = \Big[\tilde{s}_1^2 + \tilde{s}_2^2 + \tilde{s}_3^2\Big]^{1/2} - \sqrt{\frac{2}{3}}\,y(q, \varTheta)$.

(v) Associative flow rule (Perzyna model):

$$-\frac{1}{2}\mathcal{L}_v\mathbf{b}^{\mathrm{e}}\cdot[\mathbf{b}^{\mathrm{e}}]^{-1} = \frac{\dot{\gamma}}{1 - D}\left[\sum_{A=1}^{3} n_A\,\boldsymbol{\nu}^A \otimes \boldsymbol{\nu}^A\right],$$

where

$$\dot{\gamma} = \frac{1}{t_\star}\left\langle\frac{\varPhi^{\mathrm{vp}}(\tilde{s}_A, q, \varTheta)}{\kappa^{\mathrm{vp}}}\right\rangle^{1/m}, \quad \mathbf{s} = \sum_{A=1}^{3} s_A\,\boldsymbol{\nu}^A \otimes \boldsymbol{\nu}^A \quad \text{and} \quad n_A = \frac{s_A}{\|\mathbf{s}\|}.$$

(vi) Evolution equations for hardening and damage:

$$\dot{\alpha} = \dot{\gamma}\sqrt{\frac{2}{3}} \quad \text{and} \quad \dot{D} = \dot{\gamma}\frac{1}{[1 - D]^r}\left[\frac{\langle Y^{\mathrm{d}} - Y_0^{\mathrm{d}}\rangle}{a(\varTheta)}\right]^s.$$

4. Numerical implementation

4.1. Finite element formulation of the coupled initial boundary value problem

Let $\mathbf{P} := \boldsymbol{\tau}\cdot\mathbf{F}^{-\top}$ stand for the first Piola–Kirchhoff stress and $\mathbf{Q} := \mathbf{q}\cdot\mathbf{F}^{-\top}$ for the heat flux of equivalent type, analogically. The primary unknowns of the thermomechanical problem $[\mathbf{u}, \mathbf{v}, \varTheta]^{\top}$, with $\mathbf{u}$, $\mathbf{v}$ and $\varTheta$, respectively, denoting the displacement vector, velocity vector and temperature, are resolved at the global solution stage by considering the following coupled differential equation set constructed at the reference configuration:

$$\left\{\begin{array}{c}\dot{\mathbf{u}} - \mathbf{v}\\ \mathrm{Div}\,\mathbf{P} + \boldsymbol{\zeta}_0 - \rho_0\dot{\mathbf{v}}\\ c\dot{\varTheta} - \varOmega_{\mathrm{mech}} + \mathcal{H} + \mathrm{Div}\mathbf{Q} - \mathrm{R}\end{array}\right\} = \mathbf{0}. \tag{75}$$

Apart from the trivial velocity vector definition given in the first row in a residual setting, the second and third rows stand for the local equation of motion and the heat equation, respectively. $\dot{\mathbf{v}}$ is the acceleration vector and ρ_0 is the reference (initial) density which is linked to the mass density in the current configuration ρ by $\rho_0 = J\,\rho$ with the balance of mass principle. $\boldsymbol{\zeta}_0$ denotes the body forces per unit underformed volume where it is linked to the body forces per unit deformed volume $\boldsymbol{\zeta}$ via $\boldsymbol{\zeta}_0 = J\boldsymbol{\zeta}$. The boundary conditions for the problem can be listed as follows:

$$\begin{aligned}&\mathbf{u} = \overline{\mathbf{u}} \text{ at } \partial\mathfrak{B}_0^{\mathbf{u}}, \quad \overline{\mathbf{T}} = \mathbf{P}\cdot\mathbf{N} \text{ at } \partial\mathfrak{B}_0^{\sigma}, \quad \partial\mathfrak{B}_0^{\mathbf{u}} \cap \partial\mathfrak{B}_0^{\sigma} = \varnothing, \quad \partial\mathfrak{B}_0^{\mathbf{u}} \cup \partial\mathfrak{B}_0^{\sigma} = \partial\mathfrak{B}_0.\\ &\varTheta = \overline{\varTheta} \text{ at } \partial\mathfrak{B}_0^{\varTheta}, \quad \overline{\theta} = \mathbf{Q}\cdot\mathbf{N} \text{ at } \partial\mathfrak{B}_0^{\mathbf{q}} \quad \partial\mathfrak{B}_0^{\varTheta} \cap \partial\mathfrak{B}_0^{\mathbf{q}} = \varnothing, \quad \partial\mathfrak{B}_0^{\varTheta} \cup \partial\mathfrak{B}_0^{\mathbf{q}} = \partial\mathfrak{B}_0.\end{aligned} \tag{76}$$

Here, $\mathbf{N}$ is the outward unit normal to the boundary $\partial\mathfrak{B}_0$ in the reference configuration. $\partial\mathfrak{B}_0^{\mathbf{u}} \subset \partial\mathfrak{B}_0$ and $\partial\mathfrak{B}_0^{\Theta} \subset \partial\mathfrak{B}_0$ denote the parts of the boundary on which the Dirichlet boundary conditions are specified with the prescribed displacements $\overline{\mathbf{u}}$ and temperatures $\overline{\Theta}$, respectively. With the prescribed tractions $\overline{\mathbf{T}}$ and heat flux $\overline{\theta}$ Neumann-type boundary conditions act the boundary parts $\partial\mathfrak{B}_0^{\sigma} \subset \partial\mathfrak{B}_0$ and $\partial\mathfrak{B}_0^{\mathbf{q}} \subset \partial\mathfrak{B}_0$, respectively. The latter defines the heat flux entering the body through the boundary and its value can be assigned or defined by a convective or a radiation relation. In the current context, temperature increase is merely associated with the mechanical dissipation due to irreversible processes such as viscoplasticity and damage. Accordingly, the heat source and the temperature variations due to elastic loading are omitted, by canceling R and $\mathcal{H}$, respectively, to give $c\,\dot{\Theta} - \Omega_{\text{mech}} + \text{Div}\mathbf{Q} = 0$.

4.1.1. Staggered solution scheme

An isothermal staggered solution scheme is followed, where an isothermal mechanical step is followed by a thermal step on fixed configuration. With $\circ$ representing a *composition* Eq. (75) can be decomposed into the following mechanical (left) and thermal (right) steps:

$$\left[\begin{Bmatrix} \dot{\mathbf{u}} - \mathbf{v} \\ \text{Div}\,\mathbf{P} + \boldsymbol{\zeta}_0 \\ c\dot{\Theta} \end{Bmatrix} = \mathbf{0}\right] \circ \left[\begin{Bmatrix} \mathbf{v} \\ \dot{\mathbf{v}} \\ c\,\dot{\Theta} - \Omega_{\text{mech}} + \text{Div}\,\mathbf{Q} \end{Bmatrix} = \mathbf{0}\right]. \tag{77}$$

Mechanical step: In this step, for any generic field χ we have the following reduction of dependence $\chi(\epsilon, \Theta) \mapsto \chi(\epsilon)$. We consider the quasi-static limit with $\rho_0 \to 0$. Corresponding mechanical weak statement for the residual $\text{Div}\,\mathbf{P} + \boldsymbol{\zeta}_0$ is encapsulated in the following scalar valued function $G_{\varphi}(\mathbf{u}, \delta\mathbf{u})$ where $\delta\mathbf{u}$ denotes a sufficiently smooth virtual displacement field (defined in the reference configuration)

$$G_{\varphi}(\mathbf{u}, \delta\mathbf{u}) := \int_{\mathfrak{B}_0} \delta\mathbf{u}\cdot\left[\text{Div}\mathbf{P} + \boldsymbol{\zeta}_0\right] \mathrm{d}V = 0. \tag{78}$$

Noting that $\text{Div}(\delta\mathbf{u}\cdot\mathbf{P}) = \mathbf{Grad}\,\delta\mathbf{u}\colon\mathbf{P} + \delta\mathbf{u}\cdot\text{Div}\,\mathbf{P}$ and applying Gauss theorem with $\overline{\mathbf{T}} = \mathbf{P}\cdot\mathbf{N}$ we reach $\int_{\mathfrak{B}_0} \text{Div}(\delta\mathbf{u}\cdot\mathbf{P})\,\mathrm{d}V = \int_{\partial\mathfrak{B}_0^{\sigma}} \overline{\mathbf{T}}\cdot\delta\mathbf{u}\,\mathrm{d}A$, since $\delta\mathbf{u} = \mathbf{0}$ at $\partial\mathfrak{B}_0^{\varphi} = \partial\mathfrak{B}_0 \backslash \partial\mathfrak{B}_0^{\sigma}$ where $\backslash$ denotes the *complement*. Consequently, the total mechanical virtual work expression in Eq. (78) can be iterated as

$$G_{\varphi}(\mathbf{u}, \delta\mathbf{u}) := G_{\varphi}^{\text{int}}(\mathbf{u}, \delta\mathbf{u}) - G_{\varphi}^{\text{ext}}(\mathbf{u}, \delta\mathbf{u}) = 0. \tag{79}$$

Here, the components G_{φ}^{int} and G_{φ}^{ext} represent internal and external parts of the mechanical virtual work, respectively. Using $\mathbf{P} := \boldsymbol{\tau}\cdot\mathbf{F}^{-\top}$ and the symmetry of $\boldsymbol{\tau}$ to give $\mathbf{P}\colon\mathbf{Grad}\,\delta\mathbf{u} = \boldsymbol{\tau}\colon\mathbf{grad}\,\delta\mathbf{u}$, these amount to

$$G_{\varphi}^{\text{int}}(\mathbf{u}, \delta\mathbf{u}) := \int_{\mathfrak{B}_0} \boldsymbol{\tau}\colon\mathbf{grad}\,\delta\mathbf{u}\,\mathrm{d}V \quad \text{and} \quad G_{\varphi}^{\text{ext}}(\mathbf{u}, \delta\mathbf{u}) := \int_{\partial\mathfrak{B}_0^{\sigma}} \overline{\mathbf{T}}\cdot\delta\mathbf{u}\,\mathrm{d}A + \int_{\mathfrak{B}_0} \boldsymbol{\zeta}_0\cdot\delta\mathbf{u}\,\mathrm{d}V. \tag{80}$$

An iterative scheme based on Newton's method is used for the solution of problem (80) within the context of the finite element method. Accordingly, a sequence of consistently linearized problems is solved until the residual vanishes. To continue, we focus on the internal part of the mechanical virtual work. The time discrete form of internal virtual work given in Eq. (80.1) reads

$$G_{\varphi}^{\text{int}}(\mathbf{u}_{n+1}^{i}, \delta\mathbf{u}) = \int_{\mathfrak{B}_0} \boldsymbol{\tau}_{n+1}^{i}\colon\mathbf{grad}\,\delta\mathbf{u}\,\mathrm{d}V. \tag{81}$$

Linearization of G_{φ}^{int} given in Eq. (81) in direction of the displacement increment $\Delta\mathbf{u}_{n+1}^{i}$ where i represents the iteration number, i.e., $DG_{\varphi}^{\text{int}}(\mathbf{u}_{n+1}^{i}, \delta\mathbf{u})[\Delta\mathbf{u}_{n+1}^{i}]$ leads to

$$DG_{\varphi}^{\text{int}}(\mathbf{u}_{n+1}^{i}, \delta\mathbf{u})[\Delta\mathbf{u}_{n+1}^{i}] := \frac{\mathrm{d}}{\mathrm{d}\varepsilon}\bigg|_{\varepsilon=0} G_{\varphi}^{\text{int}}(\mathbf{u}_{n+1}^{i} + \varepsilon\Delta\mathbf{u}_{n+1}^{i}, \delta\mathbf{u}). \tag{82}$$

To save space, in the subsequent expressions we will drop the superscripts i and the subscripts $n+1$. Note that the virtual displacements $\delta\mathbf{u}$ are not a function of the configuration however the operator **grad** is, with $\mathbf{grad}\,\delta\mathbf{u} = \mathbf{Grad}\,\delta\mathbf{u}\cdot\mathbf{F}^{-1}$. Using this substitution for $\mathbf{grad}\,\delta\mathbf{u}$ and interchanging differentiation and integration in Eq. (82) we derive

$$DG_{\varphi}^{\text{int}}(\mathbf{u}, \delta\mathbf{u})[\Delta\mathbf{u}] = \int_{\mathfrak{B}_0} \frac{\mathrm{d}}{\mathrm{d}\varepsilon}\bigg|_{\varepsilon=0} \left[\boldsymbol{\tau}(\mathbf{u} + \varepsilon\Delta\mathbf{u})\colon\mathbf{Grad}\,\delta\mathbf{u}\cdot\mathbf{F}^{-1}(\mathbf{u} + \varepsilon\Delta\mathbf{u})\right] \mathrm{d}V. \tag{83}$$

Linearizations of $\mathbf{F}$, $\mathbf{F}^{\top}$ and $\mathbf{F}^{-1}$, respectively, represented by $D\mathbf{F}(\mathbf{u})[\Delta\mathbf{u}]$, $D\mathbf{F}^{\top}(\mathbf{u})[\Delta\mathbf{u}]$ and $D\mathbf{F}^{-1}(\mathbf{u})[\Delta\mathbf{u}]$ prove useful for successive developments and read

$$\left.\frac{\mathrm{d}}{\mathrm{d}\varepsilon}\right|_{\varepsilon=0} \mathbf{F}(\mathbf{u}+\varepsilon\Delta\mathbf{u}) = \mathbf{grad}\,\Delta\mathbf{u}\cdot\mathbf{F},$$
$$\left.\frac{\mathrm{d}}{\mathrm{d}\varepsilon}\right|_{\varepsilon=0} \mathbf{F}^{\mathsf{T}}(\mathbf{u}+\varepsilon\Delta\mathbf{u}) = \mathbf{F}^{\mathsf{T}}\cdot[\mathbf{grad}\,\Delta\mathbf{u}]^{\mathsf{T}},$$
$$\left.\frac{\mathrm{d}}{\mathrm{d}\varepsilon}\right|_{\varepsilon=0} \mathbf{F}^{-1}(\mathbf{u}+\varepsilon\Delta\mathbf{u}) = -\,\mathbf{F}^{-1}\cdot\mathbf{grad}\,\Delta\mathbf{u}. \tag{84}$$

Using $\boldsymbol{\tau}:=\mathbf{F}\cdot\mathbf{S}\cdot\mathbf{F}^{\mathsf{T}}$, where $\mathbf{S}=\mathbf{F}^{-1}\cdot\boldsymbol{\tau}\cdot\mathbf{F}^{-\mathsf{T}}$ denotes the second Piola–Kirchhoff stress tensor, together with $\mathbf{C}=\mathbf{F}^{\mathsf{T}}\cdot\mathbf{F}$ the linearization of $\boldsymbol{\tau}$, i.e., $D\boldsymbol{\tau}(\mathbf{u})[\Delta\mathbf{u}]$, reads

$$\left.\frac{\mathrm{d}}{\mathrm{d}\varepsilon}\right|_{\varepsilon=0} \left[\boldsymbol{\tau}(\mathbf{u}+\varepsilon\Delta\mathbf{u})\right] = 2\,\mathbf{F}\cdot\mathbf{F}\cdot\frac{\partial\mathbf{S}}{\partial\mathbf{C}}\cdot\mathbf{F}^{\mathsf{T}}\cdot\mathbf{F}^{\mathsf{T}}\colon \mathrm{sym}(\mathbf{grad}\,\Delta\mathbf{u}) + 2\mathbf{grad}\,\Delta\mathbf{u}\cdot\boldsymbol{\tau}. \tag{85}$$

Finally, using $J\,\mathfrak{c}_{\mathrm{MM}}:=2\,\mathbf{F}\cdot\mathbf{F}\cdot[\partial\mathbf{S}/\partial\mathbf{C}]\cdot\mathbf{F}^{\mathsf{T}}\cdot\mathbf{F}^{\mathsf{T}}$ the linearized mechanical internal virtual work can be reiterated to give

$$DG^{\mathrm{int}}_{\boldsymbol{\varphi}}(\mathbf{u},\delta\mathbf{u})[\Delta\mathbf{u}] = \int_{\mathfrak{B}_0}\mathbf{grad}\,\delta\mathbf{u}\colon J\,\mathfrak{c}_{\mathrm{MM}}\colon \mathrm{sym}(\mathbf{grad}\,\Delta\mathbf{u})\,\mathrm{d}V + \int_{\mathfrak{B}_0}\mathbf{grad}\,\delta\mathbf{u}\colon\left[\mathbf{grad}\,\Delta\mathbf{u}\cdot\boldsymbol{\tau}\right]\mathrm{d}V. \tag{86}$$

On the right-hand side, the first term is due to material stiffness and the second term is due to initial stress stiffness (or geometric stiffness). An explicit representation of $\mathbf{c}_{\mathrm{MM}}$ is given on the subsequent pages.[11] Together with the solution of this step, appropriate updates will be realized to give $[\mathbf{b}^{\mathrm{e}}_n,\,\boldsymbol{\xi}_n,\,\Theta_n]\mapsto[\check{\mathbf{b}}^{\mathrm{e}}_{n+1},\,\check{\boldsymbol{\xi}}_{n+1},\,\check{\Theta}_{n+1}]$.

Thermal Step. In this step, for any generic field χ we have the following reduction of dependence $\chi(\boldsymbol{\varepsilon},\Theta)\mapsto\chi(\Theta)$. Thermal weak statement for the residual $c\dot{\Theta}-\Omega_{\mathrm{mech}}+\mathrm{Div}\,\mathbf{Q}$ is encapsulated in the following scalar valued function $G_\Theta(\Theta,\delta\Theta)$ where $\delta\Theta$ denotes a sufficiently smooth virtual temperature field defined in the reference configuration

$$G_\Theta(\Theta,\delta\Theta):=\int_{\mathfrak{B}_0}\delta\Theta\left[c\,\dot{\Theta}-\Omega_{\mathrm{mech}}+\mathrm{Div}\,\mathbf{Q}\right]\mathrm{d}V=0. \tag{87}$$

Noting that $\mathrm{Div}(\delta\Theta\,\mathbf{Q})=\mathbf{Grad}\,\delta\Theta\cdot\mathbf{Q}+\delta\Theta\,\mathrm{Div}\,\mathbf{Q}$ and applying Gauss theorem with $\overline{\theta}=\mathbf{Q}\cdot\mathbf{N}$ we reach $\int_{\mathfrak{B}_0}\mathrm{Div}(\delta\Theta\,\mathbf{Q})\,\mathrm{d}V=\int_{\partial\mathfrak{B}^{\mathbf{q}}_0}\overline{\theta}\,\delta\Theta\,\mathrm{d}A$, since $\delta\Theta=0$ at $\partial\mathfrak{B}^{\Theta}_0=\partial\mathfrak{B}_0\backslash\partial\mathfrak{B}^{\mathbf{q}}_0$. Consequently, the total virtual work expression in Eq. (87) can be rewritten as

$$G_\Theta(\Theta,\delta\Theta):=G^{\mathrm{int}}_\Theta(\Theta,\delta\Theta)-G^{\mathrm{ext}}_\Theta(\Theta,\delta\Theta)=0. \tag{88}$$

Here, the components G^{int}_Θ and G^{ext}_Θ represent internal and external part of the thermal virtual work, respectively. Using $\mathbf{Q}=\mathbf{q}\cdot\mathbf{F}^{-\mathsf{T}}$ to give $\mathbf{Grad}\,\delta\Theta\cdot\mathbf{Q}=-\,[1-D]k\,\mathbf{grad}\,\delta\Theta\cdot\mathbf{grad}\,\Theta$ with Fourier heat conduction relation, these amount to

$$G^{\mathrm{int}}_\Theta(\Theta,\delta\Theta):=\int_{\mathfrak{B}_0}\delta\Theta\,\Omega_{\mathrm{mech}}\,\mathrm{d}V-\int_{\mathfrak{B}_0}c\,\delta\Theta\,\dot{\Theta}\,\mathrm{d}V+\int_{\mathfrak{B}_0}[1-D]k\,\mathbf{grad}\,\delta\Theta\cdot\mathbf{grad}\,\Theta\,\mathrm{d}V,$$
$$G^{\mathrm{ext}}_\Theta(\Theta,\delta\Theta):=\int_{\partial\mathfrak{B}^{\mathbf{q}}_0}\overline{\theta}\,\delta\Theta\,\mathrm{d}A. \tag{89}$$

Similar to the mechanical step, we focus on the internal part of the thermal virtual work. The time discrete form of internal virtual work given in Eq. (89.1) reads

$$G^{\mathrm{int}}_\Theta(\Theta^i_{n+1},\delta\Theta):=\int_{\mathfrak{B}_0}\delta\Theta\,\Omega^i_{\mathrm{mech},n+1}\,\mathrm{d}V-\int_{\mathfrak{B}_0}c^i_{n+1}\,\delta\Theta\,\frac{\Delta\Theta^i_{n+1}}{\Delta t}\,\mathrm{d}V+\int_{\mathfrak{B}_0}[1-D^i_{n+1}]k\,\mathbf{grad}\,\delta\Theta\cdot\mathbf{grad}\,\Theta^i_{n+1}\,\mathrm{d}V. \tag{90}$$

Linearization of G^{int}_Θ in direction of the temperature increment $\Delta\Theta^i_{n+1}$, i.e., $DG^{\mathrm{int}}_\Theta(\Theta^i_{n+1},\delta\Theta)[\Delta\Theta^i_{n+1}]$, leads to

$$DG^{\mathrm{int}}_\Theta(\Theta^i_{n+1},\delta\Theta)[\Delta\Theta]:=\left.\frac{\mathrm{d}}{\mathrm{d}\varepsilon}\right|_{\varepsilon=0}G^{\mathrm{int}}_\Theta(\Theta^i_{n+1}+\varepsilon\Delta\Theta^i_{n+1},\delta\Theta). \tag{91}$$

Like before dropping the superscripts i and the subscripts $n+1$, the linearized thermal internal virtual work expression is given as

[11] The spatial constitutive tangent moduli $c_{\mathrm{MM,ijkl}}$ can be computed with a push-forward transformation of Lagrangian constitutive tangent moduli C_{IJKL} viz.

$$J\,c_{\mathrm{MM,ijkl}}=F_{iI}F_{jJ}F_{kK}F_{lL}C_{IJKL}\quad\text{with}\quad C_{IJKL}=2\frac{\partial S_{IJ}}{\partial C_{KL}}.$$

$$DG_{\Theta}^{\mathrm{int}}(\Theta,\delta\Theta)[\Delta\Theta]=\int_{\mathfrak{B}_0}\delta\Theta\left[c_{\Theta\Theta}-\frac{\partial c}{\partial\Theta}\frac{\Delta\Theta}{\Delta t}-\frac{c}{\Delta t}\right]\Delta\Theta\,\mathrm{d}V+\int_{\mathfrak{B}_0}\left[1-D\right]k\,\mathbf{grad}\,\delta\Theta\cdot\mathbf{grad}\,\Delta\Theta\,\mathrm{d}V$$
$$-\int_{\mathfrak{B}_0}\frac{\partial D}{\partial\Theta}\Delta\Theta k\,\mathbf{grad}\,\delta\Theta\cdot\mathbf{grad}\,\Theta\,\mathrm{d}V. \tag{92}$$

Here, $c_{\Theta\Theta}:=\partial\Omega_{\mathrm{mech}}/\partial\Theta$ represents the thermoinelastic modulus. At this step, the variable update $[\check{\mathbf{b}}^{\mathrm{e}}_{n+1},\check{\boldsymbol{\xi}}_{n+1},\check{\Theta}_{n+1}]\mapsto[\mathbf{b}^{\mathrm{e}}_{n+1},\boldsymbol{\xi}_{n+1},\Theta_{n+1}]$ is realized. Accordingly, temperature change induced by inelastic dissipative mechanisms such as plasticity and damage is taken into account as well as softening and expansion induced by temperature. Besides, heat conduction is affected by deformation and damage.

4.2. Return mapping

Update of the state variables with local integration follows a two-step operator-split with a simultaneous plastic/damage correction for a given elastic prediction. Studying a strain driven process, we define an elastic trial left Cauchy–Green deformation tensor $\mathbf{b}^{\mathrm{e,tri}}$, making use of relative deformation gradient tensor at current step, i.e., $\mathbf{f}=\mathbf{F}\cdot\mathbf{F}_n^{-1}$, and elastic left Cauchy–Green deformation tensor of the previous step, i.e., $\mathbf{b}^{\mathrm{e}}_n$, as follows:

$$\mathbf{b}^{\mathrm{e,tri}}=\mathbf{f}\cdot\mathbf{b}^{\mathrm{e}}_n\cdot\mathbf{f}^{\mathrm{T}}\quad\text{where}\quad\mathbf{b}^{\mathrm{e,tri}}=\sum_{A=1}^{3}\left[\lambda_A^{\mathrm{e,tri}}\right]^2\boldsymbol{\nu}^{\mathrm{tri},A}\otimes\boldsymbol{\nu}^{\mathrm{tri},A}. \tag{93}$$

For the integration of flow rule given in Eq. (64) exponential mapping approximation which exploits the coaxiality of the plastic flow and the elastic trial state is used. Accordingly, the following plastic-damage correction on trial elastic principal strains, where the strain corrections are in the form of the principal plastic strain increments $\Delta\epsilon_A^{\mathrm{vp}}$, is carried out:

$$\epsilon_A^{\mathrm{e}}=\epsilon_A^{\mathrm{e,tri}}-\Delta\epsilon_A^{\mathrm{vp}}\quad\text{where}\quad\Delta\epsilon_A^{\mathrm{vp}}=\frac{\Delta\gamma}{1-D}\frac{\partial\Phi^{\mathrm{vp}}}{\partial\tilde{\tau}_A}, \tag{94}$$

with $\Delta\gamma=\Delta t\dot{\gamma}$. Using Eqs. (65) and (66) for $\dot{\alpha}$ and $\dot{D}$, the implicit backward-Euler method yields

$$\alpha=\alpha_n+\sqrt{\frac{2}{3}}\Delta\gamma\quad\text{and}\quad D=D_n+\Delta\gamma\frac{1}{[1-D]^r}\left[\frac{\langle Y^{\mathrm{d}}-Y_0^{\mathrm{d}}\rangle}{a(\Theta)}\right]^s. \tag{95}$$

Resultant viscoplastic/damage correction of principal Kirchhoff stresses yields

$$\tilde{\tau}_A=\tilde{\tau}_A^{\mathrm{tri}}-2\mu\frac{\Delta\gamma}{1-D}n_A\quad\text{with}\quad\tilde{\tau}_A^{\mathrm{tri}}=\tilde{p}+\tilde{s}_A^{\mathrm{tri}}. \tag{96}$$

Moreover, the viscoplastic potential at step $n+1$ reads

$$\Phi^{\mathrm{vp}}:=\|\tilde{\mathbf{s}}\|-\sqrt{\frac{2}{3}}y(q,\Theta). \tag{97}$$

Using Eq. (69), the mechanical dissipation at step $n+1$ is defined as

$$\Omega_{\mathrm{mech}}=\frac{\Delta\gamma}{\Delta t}\left[\|\tilde{\mathbf{s}}\|+\sqrt{\frac{2}{3}}q(\alpha,\Theta)+\frac{Y^{\mathrm{d}}}{[1-D]^r}\left[\frac{\langle Y^{\mathrm{d}}-Y_0^{\mathrm{d}}\rangle}{a(\Theta)}\right]^s\right]. \tag{98}$$

We apply the backward-Euler method for the integration of the components of the inelastic entropy. Accordingly, in view of Eq. (70), the viscoplastic part reads

$$\eta^{\mathrm{vp}}=\eta_n^{\mathrm{vp}}-\Delta\gamma\sqrt{\frac{2}{3}}g'_{\omega^{\mathrm{vp}}}(\Theta)\tau_{y0,0}. \tag{99}$$

Applying Eq. (71) the damage entropy is integrated to read

$$\eta^{\mathrm{d}}=\eta_n^{\mathrm{d}}-\Delta\gamma g'_{\omega^{\mathrm{d}}}(\Theta)a_0\frac{s}{s+1}\frac{1}{[1-D]^r}\left[\frac{\langle Y^{\mathrm{d}}-Y_0^{\mathrm{d}}\rangle}{a(\Theta)}\right]^{s+1}. \tag{100}$$

Eqs. (99) and (100) add up to find $\eta^{\mathrm{vpd}}=\eta^{\mathrm{vp}}+\eta^{\mathrm{d}}$. It is remarkable that the local integration expressions for η^{vp} and η^{d} have explicit representations in $\Delta\gamma$ and D. Thus, setting the inelastic entropy as an additional internal variable does not alter the local integration scheme and conventional finite thermoplastic algorithmic structure presented in Simó and Miehe (1992), even for damage-coupled conditions.

4.2.1. Solution of equations of local integration

Following Simó and Taylor (1985), local governing equations collected so far can be reduced, particularly for the chosen yield criterion, making use of the substitution $\tilde{s}_A = \|\tilde{\mathbf{s}}\| n_A$ and exploiting the condition of collinear flow and the trial Kirchhoff stress tensor, finally, representing the hardening/softening function definition in terms of the viscoplastic multiplier, to reach

$$\mathbf{r}(\mathbf{x}) = \left\{ \begin{array}{c} \sqrt{\frac{2}{3}}\left[\tau_{y0}(\Theta) - q\left(\alpha_n + \sqrt{\frac{2}{3}}\Delta\gamma, \Theta \right) \right] - \|\tilde{\mathbf{s}}^{\mathrm{tri}}\| + 2\mu\frac{\Delta\gamma}{1-D} + \kappa^{\mathrm{vp}}\left[\frac{t_\star \Delta\gamma}{\Delta t} \right]^m \\ D - D_n - \Delta\gamma \frac{1}{[1-D]^r}\left[\frac{\langle Y^{\mathrm{d}} - Y_0^{\mathrm{d}} \rangle}{a(\Theta)} \right]^s \end{array} \right\}, \tag{101}$$

where $\mathbf{r} = \mathbf{r}(\mathbf{x}) = \mathbf{0}$. The array of unknowns is represented by $\mathbf{x} = [\Delta\gamma, D]^{\mathrm{T}}$. Eqs. (101) can be treated with the standard Newton–Raphson solution scheme. Accordingly, the linearized version of the equations is given as $\mathrm{d}\mathbf{r} = \boldsymbol{\Gamma}\cdot\mathrm{d}\mathbf{x}$, where $\boldsymbol{\Gamma}$ denotes the Jacobian of the system

$$\boldsymbol{\Gamma} = \begin{bmatrix} \frac{\partial r_1}{\partial \Delta\gamma} & \frac{\partial r_1}{\partial D} \\ \frac{\partial r_2}{\partial \Delta\gamma} & \frac{\partial r_2}{\partial D} \end{bmatrix}, \tag{102}$$

where the component derivations are given in Appendix A. Using $\boldsymbol{\Gamma}^{-1}\cdot\mathrm{d}\mathbf{r} = \mathrm{d}\mathbf{x}$, the solution for $\mathbf{x}$, which constitutes the local return mapping realized at each Gauss point, is found via the iterative scheme

$$\mathbf{x}^{(k+1)} = \mathbf{x}^{(k)} - \delta^{(k)}[\boldsymbol{\Gamma}^{(k)}]^{-1}\cdot\mathbf{r}^{(k)}, \tag{103}$$

where k represents the iteration number and $\delta^{(k)} \in (0, 1]$ is the proper line-search parameter.

4.3. Algorithmic tangent matrices

For the monolithic solution of the global equilibrium problem of coupled thermomechanical analysis, one has

$$\mathbf{r} = \mathbf{r}(\hat{\mathbf{x}}) = \mathbf{0}; \quad \hat{\mathbf{x}} = \left\{ \begin{array}{c} \epsilon_B \\ \Theta \\ \Delta\gamma \\ D \end{array} \right\} \quad \text{for } B = 1, 2, 3, \tag{104}$$

where $\Delta\gamma = \Delta\gamma(\boldsymbol{\epsilon}, \Theta)$ and $D = D(\boldsymbol{\epsilon}, \Theta)$. A mechanical–thermal staggered approach introduces the following simplifications into the solution scheme.

Mechanical step: For the mechanical step $\mathbf{c}_{\mathrm{MM}}$ reads

$$J\mathfrak{c}_{\mathrm{MM}} = \sum_{A=1}^{3}\sum_{B=1}^{3} a_{AB}^{\mathrm{evpd}} \boldsymbol{\Lambda}^{\mathrm{tri},AABB} - \sum_{A=1}^{3} 2\tau_A \boldsymbol{\Lambda}^{\mathrm{tri},AAAA} + \sum_{A=1}^{3}\sum_{\substack{B=1 \\ A\neq B}}^{3} \vartheta_{AB}\left[\boldsymbol{\Lambda}^{\mathrm{tri},ABAB} + \boldsymbol{\Lambda}^{\mathrm{tri},ABBA} \right]. \tag{105}$$

a_{AB}^{evpd} corresponds to the following 3×3 matrix:

$$a_{AB}^{\mathrm{evpd}} = \frac{\partial \tau_A}{\partial \epsilon_B} \equiv \frac{\partial \tau_A}{\partial \epsilon_B^{\mathrm{e,tri}}}, \tag{106}$$

where the condition $\partial[\bullet]/\partial\epsilon_B \equiv \partial[\bullet]/\partial\epsilon_B^{\mathrm{e,tri}}$ is exploited. $\boldsymbol{\Lambda}^{ABCD}$ represents a fourth-order tensor with $\boldsymbol{\Lambda}^{ABCD} := \boldsymbol{\nu}^A \otimes \boldsymbol{\nu}^B \otimes \boldsymbol{\nu}^C \otimes \boldsymbol{\nu}^D$. The designation of ϑ_{AB} is given as[12]

$$\vartheta_{AB} = \frac{\tau_A\left[\lambda_B^{\mathrm{e,tri}} \right]^2 - \tau_B\left[\lambda_A^{\mathrm{e,tri}} \right]^2}{\left[\lambda_A^{\mathrm{e,tri}} \right]^2 - \left[\lambda_B^{\mathrm{e,tri}} \right]^2}. \tag{107}$$

Mechanical pass is realized under constant temperature, where $\Theta = \check{\Theta}$ which results in $\Delta\gamma = \Delta\gamma(\boldsymbol{\epsilon})|_{\Theta=\check{\Theta}}$ and $D = D(\boldsymbol{\epsilon})|_{\Theta=\check{\Theta}}$. For this stage

[12] Eq. (107) suffers from singularity or ill-conditioning for equal or nearly equal eigenvalues, respectively, where $\lambda_A^{\mathrm{e,tri}} - \lambda_B^{\mathrm{e,tri}} \to 0$. Ogden (1984, pp. 338–341) includes an analytical treatment of such cases in the context of finite elasticity materializing L'Hospital rule. In this work, a numerical perturbation as an efficient substitute for the L'Hospital rule is used. Consequently, equal or numerically close eigenvalues with $\lambda_A^{\mathrm{e,tri}} \simeq \lambda_B^{\mathrm{e,tri}}$ are perturbed with a perturbation factor $\varepsilon^{\mathrm{per}} \ll 1$ ($\varepsilon^{\mathrm{per}} = 10^{-12}$ constitutes a reasonable choice) which gives $\lambda_A^{\mathrm{e,tri}} \mapsto [1 + \varepsilon^{\mathrm{per}}]\lambda_A^{\mathrm{e,tri}}$, $\lambda_B^{\mathrm{e,tri}} \mapsto [1 - \varepsilon^{\mathrm{per}}]\lambda_B^{\mathrm{e,tri}}$, and for volumetric consistency $\lambda_C^{\mathrm{e,tri}} \mapsto 1/[[1 + \varepsilon^{\mathrm{per}}][1 - \varepsilon^{\mathrm{per}}]]\lambda_C^{\mathrm{e,tri}}$ (Miehe, 1994).

$$\mathbf{r} = \mathbf{r}(\hat{\mathbf{x}}) = \mathbf{0} \quad \text{where} \quad \hat{\mathbf{x}} = \left\{ \begin{array}{c} \epsilon_B \\ \Delta\gamma \\ D \end{array} \right\} \Bigg|_{\Theta=\check{\Theta}} . \tag{108}$$

Hence, the mechanical step in the staggered approach assumes

$$\boldsymbol{\tau}(\boldsymbol{\epsilon},\, \Theta,\, \Delta\gamma(\boldsymbol{\epsilon},\, \Theta),\, D(\boldsymbol{\epsilon},\, \Theta)) \mapsto \boldsymbol{\tau}(\boldsymbol{\epsilon},\, \Delta\gamma(\boldsymbol{\epsilon}),\, D(\boldsymbol{\epsilon}))\big|_{\Theta=\check{\Theta}}. \tag{109}$$

This allows the computation of a_{AB}^{evpd} through the chain rule

$$\frac{\partial \tau_A}{\partial \epsilon_B^{\text{e,tri}}} = \frac{\partial \tau_A}{\partial \epsilon_B^{\text{e,tri}}}\Bigg|_{\Delta\gamma, D \nrightarrow \text{const.}} + \frac{\partial \tau_A}{\partial \Delta\gamma}\frac{\mathrm{d}\Delta\gamma}{\mathrm{d}\epsilon_B^{\text{e,tri}}} + \frac{\partial \tau_A}{\partial D}\frac{\mathrm{dD}}{\mathrm{d}\epsilon_B^{\text{e,tri}}}, \tag{110}$$

where determination of $\mathrm{d}\Delta\gamma/\mathrm{d}\epsilon_B^{\text{e,tri}}$ and $\mathrm{dD}/\mathrm{d}\epsilon_B^{\text{e,tri}}$ requires the condition $\mathrm{d}\mathbf{r} = \mathbf{0}$ with

$$\left\{ \begin{array}{c} \dfrac{\mathrm{d}\Delta\gamma}{\mathrm{d}\epsilon_B} \\ \dfrac{\mathrm{dD}}{\mathrm{d}\epsilon_B} \end{array} \right\} = -\,\boldsymbol{\Gamma}^{-1}.\left\{ \begin{array}{c} \dfrac{\partial r_1}{\partial \epsilon_B} \\ \dfrac{\partial r_2}{\partial \epsilon_B} \end{array} \right\} \tag{111}$$

with $\partial[\bullet]/\partial\epsilon_B \equiv \partial[\bullet]/\partial\epsilon_B^{\text{e,tri}}$. The details of the derivations are given in Appendix B.

Thermal step: Eq. (98) is used in computation of the thermoinelastic coupling modulus $c_{\Theta\Theta}$ viz.

$$c_{\Theta\Theta} := \frac{\partial \Omega_{\text{mech}}}{\partial \Theta}. \tag{112}$$

During thermal pass the configuration is held fixed $\epsilon_A = \check{\epsilon}_A$, which results in $\Delta\gamma = \Delta\gamma(\Theta)|_{\epsilon=\check{\epsilon}}$ and $D = D(\Theta)|_{\epsilon=\check{\epsilon}}$. Consequently, one has

$$\mathbf{r} = \mathbf{r}(\hat{\mathbf{x}}) = \mathbf{0} \quad \text{where} \quad \hat{\mathbf{x}} = \left\{ \begin{array}{c} \Theta \\ \Delta\gamma \\ D \end{array} \right\} \Bigg|_{\epsilon_A=\check{\epsilon}_A} . \tag{113}$$

Hence, analogous to mechanical step one has

$$\Omega_{\text{mech}}(\boldsymbol{\epsilon},\, \Theta,\, \Delta\gamma(\boldsymbol{\epsilon},\, \Theta),\, D(\boldsymbol{\epsilon},\, \Theta)) \mapsto \Omega_{\text{mech}}(\Theta,\, \Delta\gamma(\Theta),\, D(\Theta))\big|_{\epsilon=\check{\epsilon}}. \tag{114}$$

Table 1
Material parameters for a steel-like material at reference temperature.

Parameter	Symbol	Magnitude	Dimension
Referential density	ρ_0	7.8×10^{-9}	$\mathrm{Ns^2/mm^4}$
Bulk modulus	H	164206.0	MPa
Shear modulus	μ	80193.8	MPa
Linear hardening	K_0	129.24	MPa
Flow stress	$\tau_{y,0}$	450.0	MPa
Saturation stress	$\tau_{y\infty,0}$	715.0	MPa
Saturation exponent	δ	16.93	–
Damage multiplier	a_0	5.0	MPa
Damage exponent 1	s	1.0	–
Damage exponent 2	r	2.0	–
Threshold for Y	Y_0^{d}	0	MPa
Rate exponent	m	1	–
Drag stress	κ^{vp}	100	MPa
Characteristic time	$t_\star$	1	s
Coefficient of thermal expansion	α_Θ	1.0×10^{-5}	$\mathrm{K^{-1}}$
Specific heat capacity	c_s	0.46×10^{9}	$\mathrm{mm/s^2\,K}$
Heat conductivity	k	45.0	N/sK
Plastic thermal softening	ω^{vp}	1	–
Damage thermal softening	ω^{d}	1	–
Reference temperature	Θ_0	293	K
Melting temperature	Θ_{melt}	1700	K

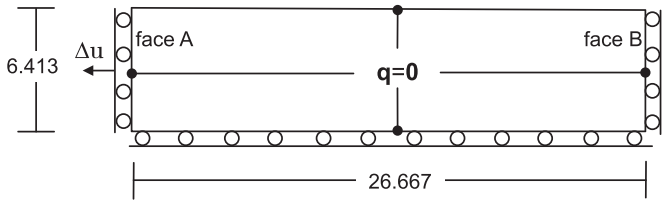

Fig. 1. Geometry and boundary conditions for tensile tests (all dimensions are in mm).

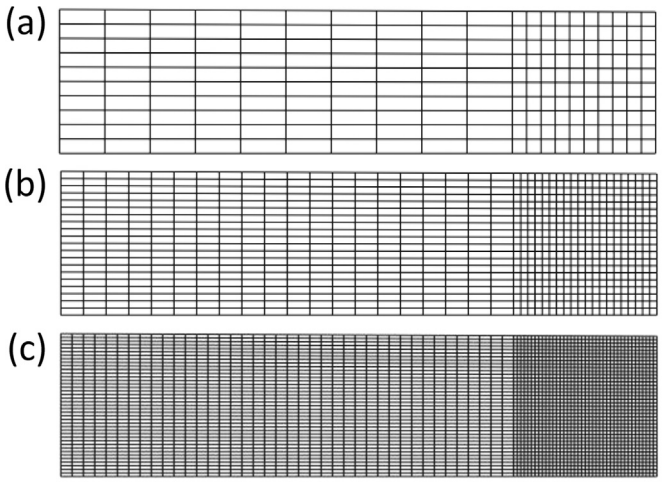

Fig. 2. Finite element meshes: (a) 10×20, (b) 20×40 and (c) 40×80.

This allows the computation of $c_{\Theta\Theta}$ with the following chain rule of differentiation:

$$\frac{\partial \Omega_{\text{mech}}}{\partial \Theta} = \frac{\partial \Omega_{\text{mech}}}{\partial \Theta}\bigg|_{\Delta\gamma, D \nrightarrow \text{const.}} + \frac{\partial \Omega_{\text{mech}}}{\partial \Delta\gamma}\frac{\mathrm{d}\Delta\gamma}{\mathrm{d}\Theta} + \frac{\partial \Omega_{\text{mech}}}{\partial D}\frac{\mathrm{dD}}{\mathrm{d}\Theta}. \tag{115}$$

where determination of $\mathrm{d}\Delta\gamma/\mathrm{d}\Theta$ and $\mathrm{d}D/\mathrm{d}\Theta$ requires the condition $\mathrm{d}\mathbf{r} = \mathbf{0}$ with

$$\begin{Bmatrix} \dfrac{\mathrm{d}\Delta\gamma}{\mathrm{d}\Theta} \\ \dfrac{\mathrm{dD}}{\mathrm{d}\Theta} \end{Bmatrix} = -\,\boldsymbol{\Gamma}^{-1} \cdot \begin{Bmatrix} \dfrac{\partial r_1}{\partial \Theta} \\ \dfrac{\partial r_2}{\partial \Theta} \end{Bmatrix}. \tag{116}$$

The details of the derivations are given in Appendix C. It should be noted that in both the mechanical pass and the thermal pass the internal variables are changing. The thermal part will be due only if there exists plastic flow and induced damage. This concludes the numerical setup.

5. Application problems

Preceding algorithmic resolutions are implemented as ABAQUS subroutines where the implementation details are included in appendices. Material parameters used in the analyses are given in Table 1, where for mere thermoplasticity the damage deterioration effects are omitted. Two example problems consisting of necking of an axisymmetric bar and localization in a 3D rectangular bar are investigated.

5.1. Necking of an axisymmetric bar

Necking of an axisymmetric bar is investigated in the context of damage-coupled thermoplastic framework. Contrary to the common idea, in the FE simulations with a typical free contracting (shear-free grip conditions) tensile test specimen of a certain gauge length, central refinement of the mesh does not suffice to transform the bifurcation problem, where the necking can emanate at any section, to a limit load problem. This is due to the fact that necking emanation requires the

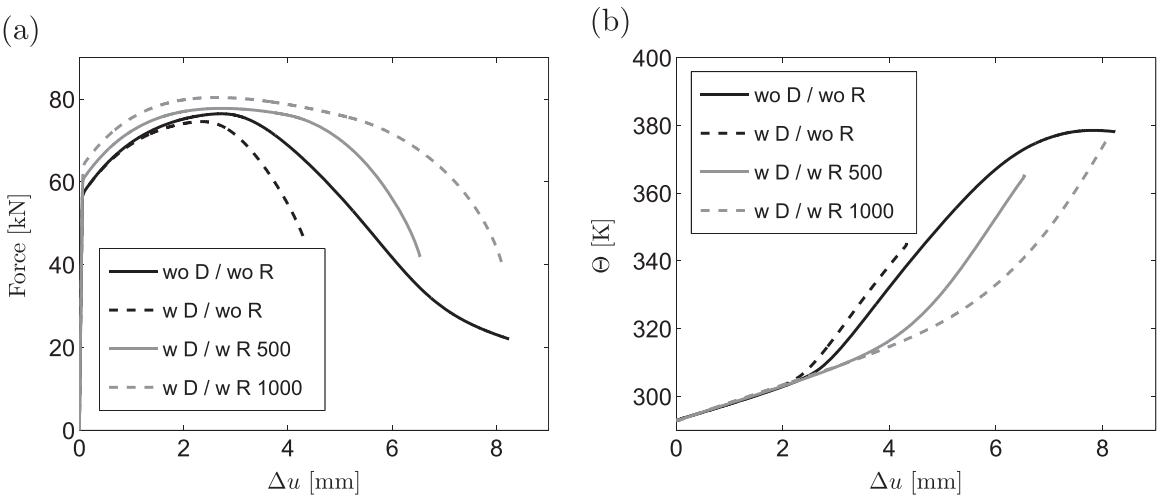

Fig. 3. History plots for axisymmetric tension problem for 10×20 mesh: (a) Load–displacement curves and (b) temperature evolution at the central node. The codes wo D and w D stand for without and with damage effect, respectively. The codes wo R, w R 500 and w R 1000 stand for without rate effect, with rate effect with $\kappa^{vp} = 500$ MPa and with rate effect with $\kappa^{vp} = 1000$ MPa, respectively.

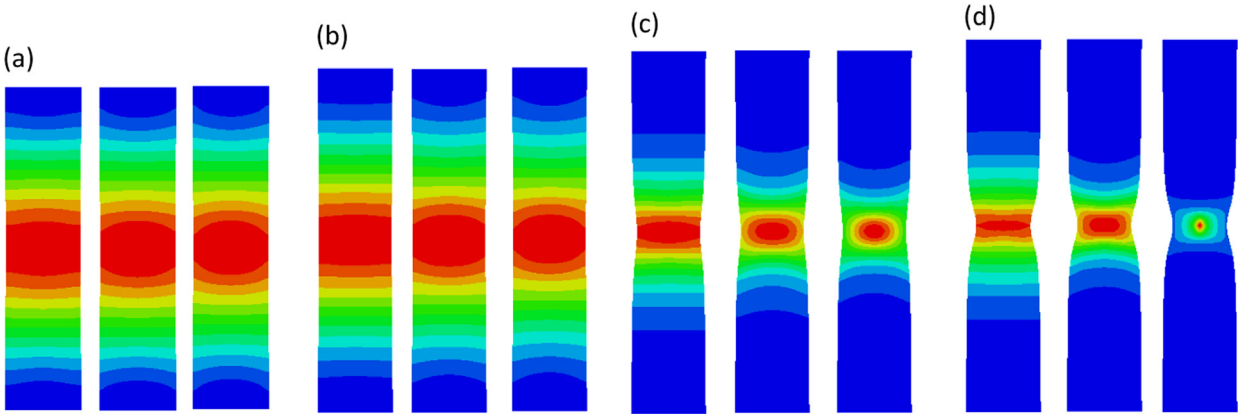

Fig. 4. Contour plots of temperature Θ, hardening strain-like variable α and damage D distribution at different displacements for damage-coupled 2D axisymmetric bar tension problem for 10×20 mesh and rate independent solution. (a) $\Delta u = 2 \times 0.25$ mm, min/max $\Theta = 293.6/294.1$, min/max $\alpha = 5.095 \times 10^{-3}/9.014 \times 10^{-3}$, min/max $D = 6.387 \times 10^{-4}/1.190 \times 10^{-3}$, (b) $\Delta u = 2 \times 2.00$ mm, min/max $\Theta = 300.3/303.2$, min/max $\alpha = 5.686 \times 10^{-2}/8.368 \times 10^{-2}$, min/max $D = 1.023 \times 10^{-2}/1.707 \times 10^{-2}$, (c) $\Delta u = 2 \times 3.50$ mm, min/max $\Theta = 301.1/328.8$, min/max $\alpha = 6.086 \times 10^{-2}/3.741 \times 10^{-1}$, min/max $D = 1.115 \times 10^{-2}/1.434 \times 10^{-1}$, and (d) $\Delta u = 2 \times 4.325$ mm, min/max $\Theta = 301.3/347.2$, min/max $\alpha = 6.086 \times 10^{-2}/6.541 \times 10^{-1}$, min/max $D = 1.115 \times 10^{-2}/9.872 \times 10^{-1}$.

break up of the stress uniformity. For this purpose, two necking triggering methods widely used in the literature are the geometric imperfection method and the thermal triggering method. The former requires a reduction of the central area, linearly varied over the half-length as utilized in Steinmann et al. (1994), Simó (1992) and Ibrahimbegović and Gharzeddine (1999), among others. In the latter, fixed temperature boundary conditions applied at both ends are utilized as a necking triggering mechanism, which was first studied by Wriggers et al. (1992).

In this first example we use the former method of introduction of a geometrical imperfection at the center. Only a quarter of the specimen has been discretized by exploiting the symmetry of the problem. Fig. 1 shows the geometrical setup and boundary conditions. In the geometrical imperfection method the radius of face B is selected as 98.2% of the radius of face A. The heat exchange at the surfaces of the specimen are neglected by assuming adiabatic thermal boundary conditions. A displacement controlled simulation is performed where the displacement Δu is assigned to face A as seen in Fig. 1b with a loading rate of 1 mm/s. The elements are assumed to have a reference absolute temperature of $\Theta_0 = 293$ K.

In order to evaluate the mesh dependence of the softening mechanism due to temperature and damage and the effect of viscosity we use 10×20, 20×40 and 40×80 meshes as shown in Fig. 2a, b and c, respectively. Here 10×20 refers to 10 elements in radial direction and 20 elements in longitudinal direction. The meshes are composed of element CAX4T, which is a 4-node axisymmetric thermally coupled quadrangular element with bilinear displacement and temperature

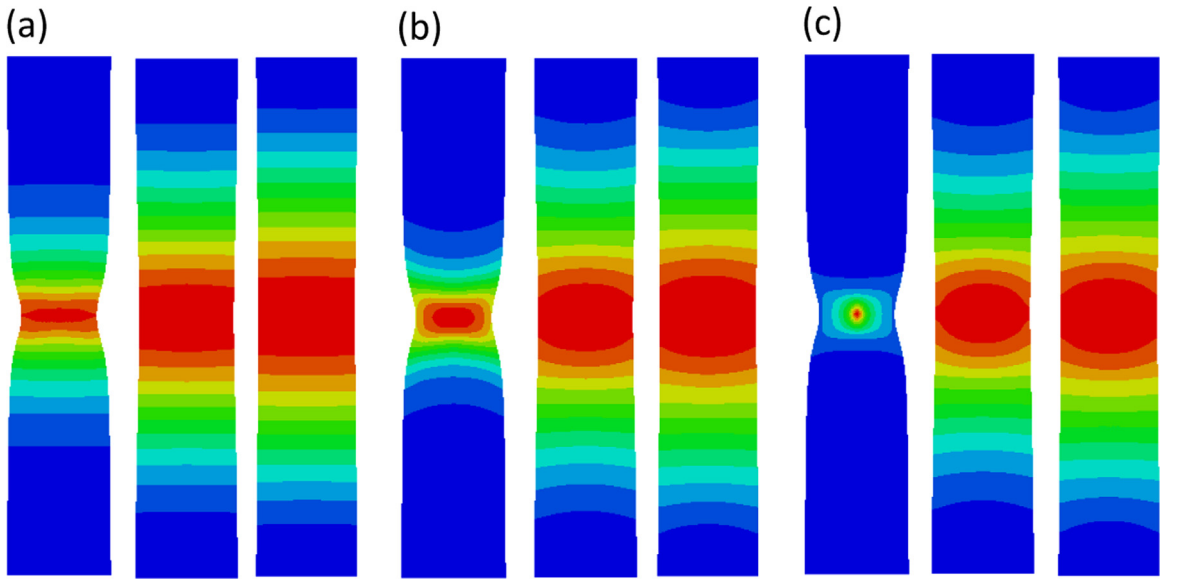

Fig. 5. Contour plots of temperature Θ, hardening strain-like variable α and damage D distributions at $\Delta u = 2 \times 0.25$ mm for damage-coupled 2D axisymmetric bar tension problem for 10×20 mesh and for $\kappa^{\mathrm{vp}} = 0$ (left), $\kappa^{\mathrm{vp}} = 500$ (center) and $\kappa^{\mathrm{vp}} = 1000$ (right). (a) min/max (left) $\Theta = 301.3/347.2$, (center) $\Theta = 306.5/320.4$, (right) 309.7/317.0, (b) min/max (left) $\alpha = 6.086 \times 10^{-2}/6.541 \times 10^{-2}$, (center) $\alpha = 9.697 \times 10^{-2}/2.157 \times 10^{-1}$, (right) $\alpha = 1.173 \times 10^{-2}/1.763 \times 10^{-1}$, and (c) min/max (left) $D = 1.115 \times 10^{-2}/9.872 \times 10^{-1}$, (center) $D = 2.187 \times 10^{-2}/6.712 \times 10^{-2}$, (right) $D = 3.001 \times 10^{-2}/5.466 \times 10^{-2}$.

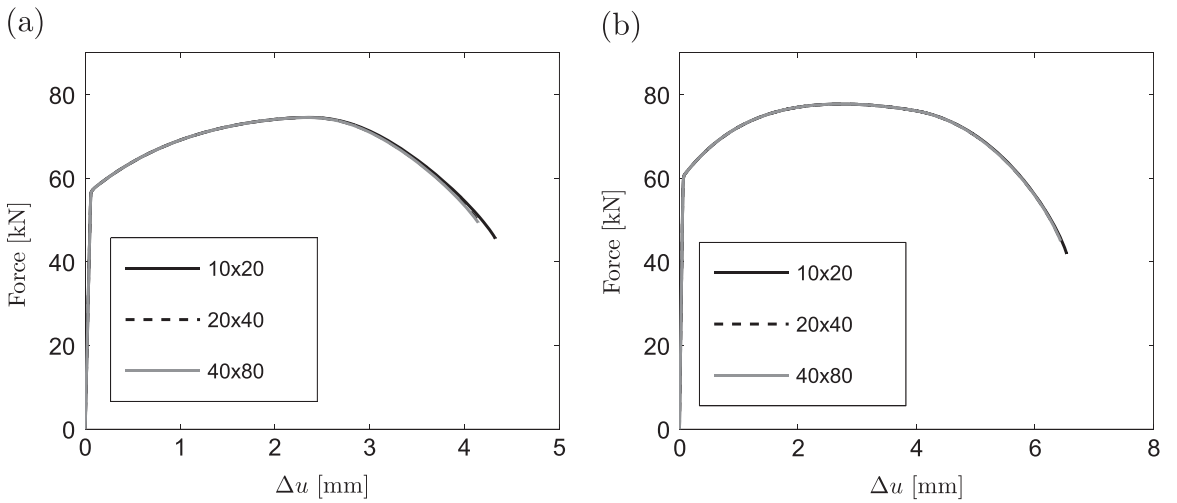

Fig. 6. Load–displacement curves for 10×20, 20×40 and 40×80 discretizations. (a) Rate independent solution with $\kappa^{\mathrm{vp}} = 0$. (b) Rate dependent solution with $\kappa^{\mathrm{vp}} = 500$ MPa.

interpolations. Besides rate independent limit with $\kappa^{\mathrm{vp}} = 0$, rate effects are also investigated taking $\kappa^{\mathrm{vp}} = 500$ MPa and $\kappa^{\mathrm{vp}} = 1000$ MPa.[13]

Considering damage evolution and mesh with 10×20 discretization, the load–displacement and the central temperature increment history plots are given in Fig. 3a and b, respectively. The initiation of the necking is signaled by the peak of the load deflection curves. The figures clearly reveal the effect of damage where in the absence of damage the neck is slightly delayed. Moreover, the abrupt loss in the load carrying capacity together with necking is precluded in the simulations where rate effects are considered. For the central temperature evolution, more rapid confinement of the plastic zone to the necked area in the middle of the bar in the absence of rate affects results in a stronger raise in temperature at the specimen center.

Contour plots of temperature Θ, hardening strain-like variable α and damage D distribution at different displacements for damage-coupled 2D axisymmetric bar tension problem for 10×20 mesh and rate dependent solution are given in Fig. 4. With neck development there occurs considerable temperature increase with inelastic dissipation. Also the central damage

[13] In the most general case, instantaneous elasticity and inviscid plasticity bound the expansion of the damage affected yield surface with $0 \leq \kappa^{\mathrm{vp}} < \infty$.

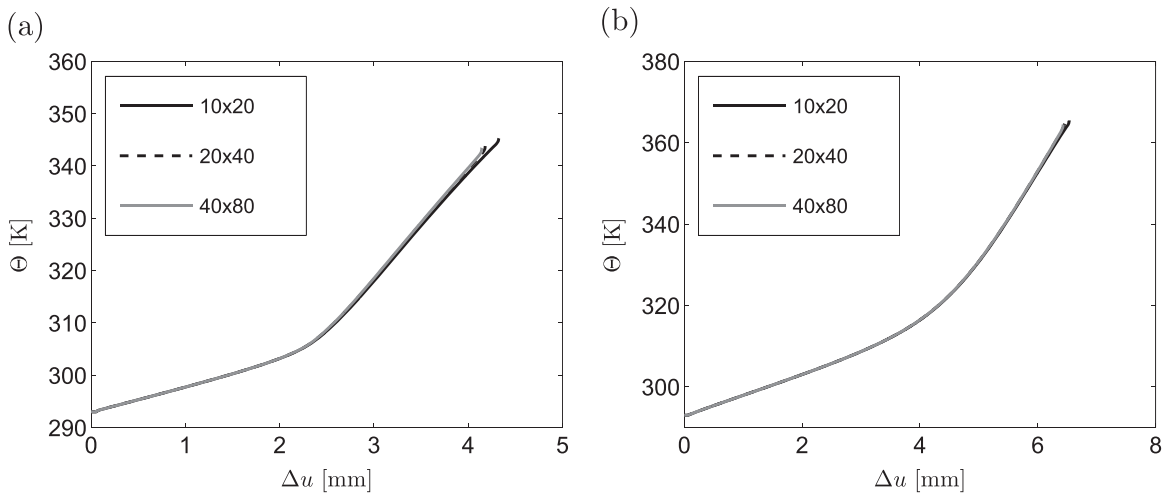

Fig. 7. Central temperature development with self-heating for 10×20, 20×40 and 40×80 discretizations. (a) Rate independent solution with $\kappa^{vp} = 0$. (b) Rate dependent solution with $\kappa^{vp} = 500$ MPa.

localization is more noticeable as compared to other fields. This is primarily due to the increased stress triaxiality ratio at the specimen center and it is in agreement with experimentally observed cup and cone fracture. Since the minimum of the hardening variable and damage ceases to evolve at latter stages we understand that elastic unloading takes place in a considerable part of the specimen.

Fig. 5 depicts the effect of viscosity on development of inelastic fields and temperature. In agreement with the given load–displacement plots, inclusion of rate affects delays neck formation and hence associated inelastic dissipation at the center whereas in the inviscid solution there occurs considerable damage development. Hence, a more concentrated plastic zone and a sharper curvature of the neck than the viscous results is observed. Together with the inclusion of viscosity, localized behavior of the rate independent analyses diffuse; that is, the deformation localized at the elements of the central band is distributed to a wider band. This also decreases the radius reduction at the center. In the inviscid analyses, intensities of both the maximum equivalent plastic strain and the temperature are higher than those of viscous analysis.

The mesh dependence of the doubly induced softening mechanism due to temperature and damage is tested together by considering the effect of viscosity for $\kappa^{vp} = 500$ MPa. Fig. 6a and b shows load–displacement curves for inviscid and viscous solutions, respectively. Although in both of the cases the mesh effect is considerably small, in the inviscid case, a more noticeable branching among solutions starting just after the peak is observed. For the rate dependent solution this branching seems to be further bypassed. This is parallel to the observations in the literature on viscous regularization (Wang et al., 1997). The difference in responses for 10×20 and 20×40 meshes could be attributed to the rather coarse nature of 10×20 mesh,

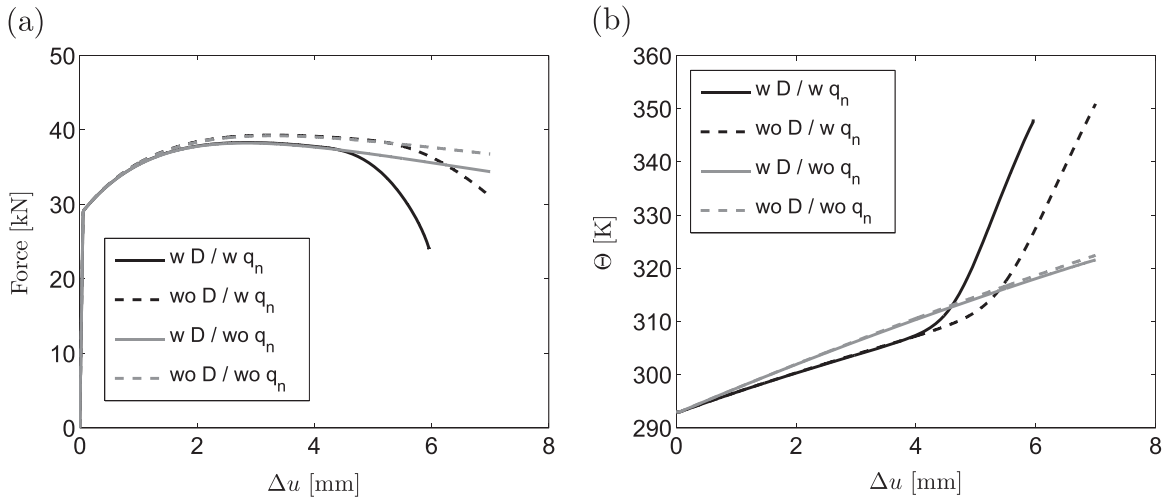

Fig. 8. (a) Load–displacement curves for rate dependent solutions with and without damage and heat convection at free surfaces. (b) Development of temperature at central node for rate dependent solutions with and without damage and heat convection at free surfaces. In (a) and (b), the identifiers w D and wo D stand for with and without damage, respectively, whereas the identifiers w q_n and wo q_n, respectively, denote with and without heat convection at free surface.

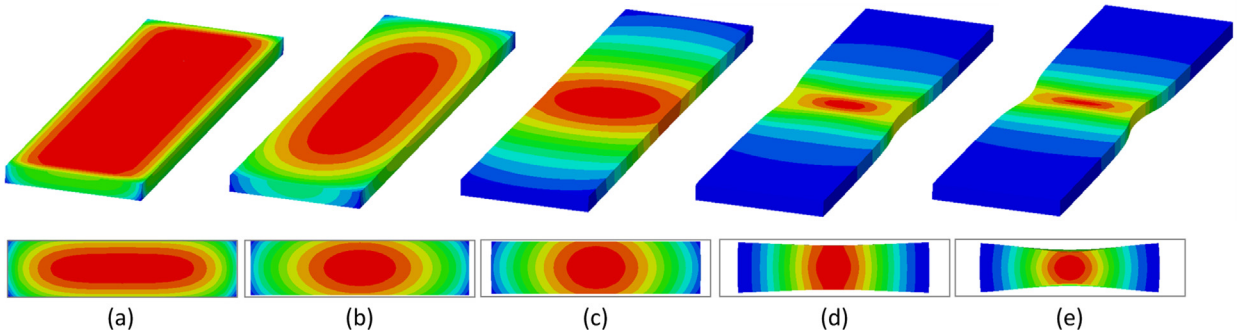

Fig. 9. Contour plots of temperature distribution at different displacements for damage-coupled 3D rectangular bar tension problem rate dependent solution. At top, distributions over the central plane along the plate plane are shown. At the bottom, central transverse section distributions are given. The outer frame denotes the undeformed shape to highlight the amount of deformation by necking. (a) $\Delta u = 2 \times 0.25$ mm, min/max $\Theta = 293.1/293.8$ K, (b) $\Delta u = 2 \times 2.75$ mm, min/max $\Theta = 301.4/302.9$ K, (c) $\Delta u = 2 \times 4.50$ mm, min/max $\Theta = 304.4/311.5$ K, (d) $\Delta u = 2 \times 5.45$ mm, min/max $\Theta = 303.6/334.8$ K, and (e) $\Delta u = 2 \times 5.96$ mm, min/max $\Theta = 303.2/349.9$ K.

hence classical mesh dependence of finite element solutions. Further differences with mesh refinement, however, are due to damage. In the rate independent solution, together with the refined mesh the analysis is terminated earlier at smaller deformations. Besides, the post-peak response has a sharper decrease compared to the rate dependent solution where a rather diffuse localization is observed.

Fig. 7a and b shows central temperature development for inviscid and viscous solutions for different mesh refinement levels. In agreement with Fig. 6 the central localization of temperature with further mesh refinement for the regularized solution is not as strong as the regularized one.

5.2. Localization of rectangular bar

In this 3D example, we investigate the localization in a rectangular bar with the geometry width/thickness/length = 16/4/52 mm. This problem was studied in Simó and Miehe (1992) in the absence of damage. Contraction-free boundary conditions are applied during displacement controlled tensile loading of the bar. Since no geometrical imperfections are introduced, these boundary conditions result in a homogeneous state of stress throughout the loading. In order to trigger neck, thermal boundary conditions are arranged as to account for convective heat exchange on the entire free surface of the specimen (except for the symmetry surfaces) given by the expression $q_n = h[\Theta_\infty - \Theta]$. Here, $h = 17.5 \times 10^{-3}$ N/m m s K denotes the convection coefficient and $\Theta_\infty = 293$ K represents the temperature of the surrounding (infinite) medium. With self-heating by mechanical dissipation, an uneven temperature distribution, and, hence inhomogeneous stress distribution occurs over the specimen. Thus, necking develops.

Only one-eighth of the specimen is modeled using the symmetry in loading as well as geometry. Discretization of the modeled part consists of 1280 8-node full integration temperature displacement elements of type C3D8T with trilinear displacement and temperature interpolations. Like before, the loading is applied under constant velocity with 1 mm/s. The analyses are conducted for damage coupled and uncoupled cases with viscosity parameter $\kappa^{vp} = 100$ MPa. Except for this, the material parameters are the ones given in Table 1. For comparison reasons cases without heat convection, i.e., homogeneous solutions, are also accounted for.

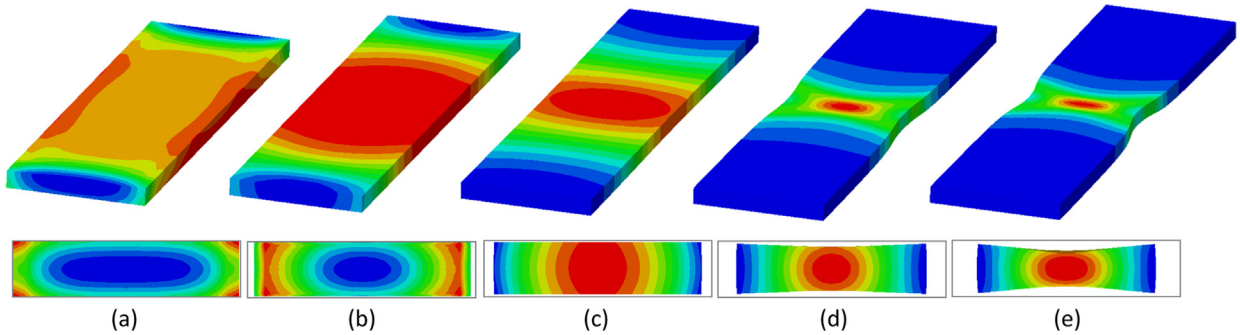

Fig. 10. Contour plots of hardening strain-like variable α distribution at different displacements for damage-coupled 3D rectangular bar tension problem rate dependent solution. At top, distributions over central plane along plate plane are shown. At the bottom, central transverse section distributions are given. The outer frame denotes the undeformed shape to highlight the amount of deformation by necking. (a) $\Delta u = 2 \times 0.25$ mm, min/max $\alpha = 7.199 \times 10^{-3}/7.210 \times 10^{-3}$, (b) $\Delta u = 2 \times 2.75$ mm, min/max $\alpha = 9.576 \times 10^{-2}/9.650 \times 10^{-2}$, (c) $\Delta u = 2 \times 4.50$ mm, min/max $\alpha = 1.330 \times 10^{-1}/1.789 \times 10^{-1}$, (d) $\Delta u = 2 \times 5.45$ mm, min/max $\alpha = 1.333 \times 10^{-1}/4.609 \times 10^{-1}$, and (e) $\Delta u = 2 \times 5.96$ mm, min/max $\alpha = 1.333 \times 10^{-1}/7.378 \times 10^{-1}$.

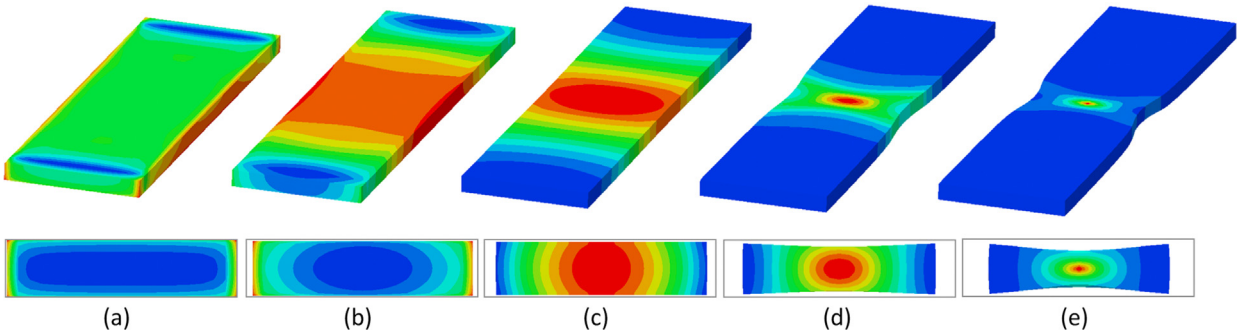

Fig. 11. Contour plots of damage D distribution at different displacements for damage-coupled 3D rectangular bar tension problem rate dependent solution. At top, distributions over central plane along plate plane are shown. At the bottom, central transverse section distributions are given. The outer frame denotes the undeformed shape to highlight the amount of deformation by necking. (a) $\Delta u = 2 \times 0.25$ mm, min/max $D = 9.500 \times 10^{-4}/9.527 \times 10^{-4}$, (b) $\Delta u = 2 \times 2.75$ mm, min/max $D = 2.064 \times 10^{-2}/2.086 \times 10^{-2}$, (c) $\Delta u = 2 \times 4.50$ mm, min/max $D = 3.185 \times 10^{-2}/4.686 \times 10^{-2}$, (d) $\Delta u = 2 \times 5.45$ mm, min/max $D = 3.185 \times 10^{-2}/1.910 \times 10^{-1}$, and (e) $\Delta u = 2 \times 5.96$ mm, min/max $D = 3.185 \times 10^{-2}/9.948 \times 10^{-1}$.

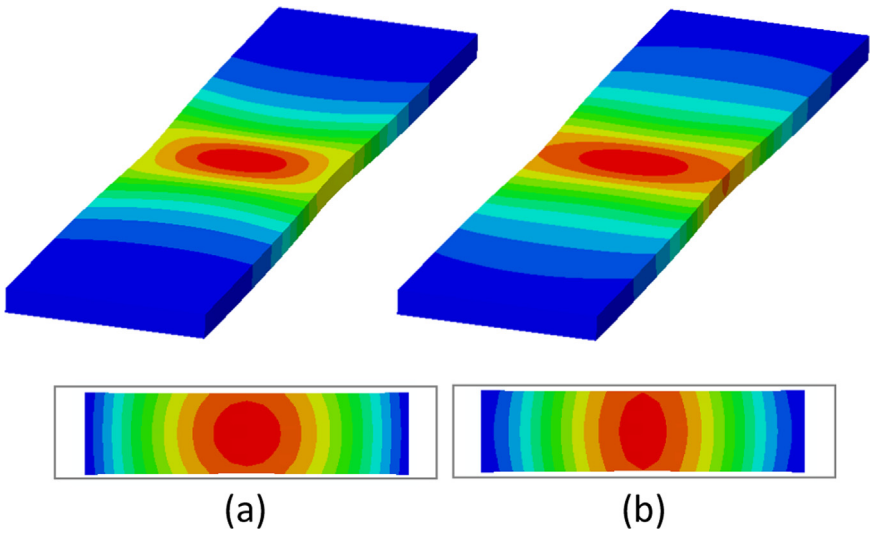

Fig. 12. Contour plots of (a) hardening strain-like variable α and (b) temperature distribution at $\Delta u = 2 \times 5.96$ mm for 3D rectangular bar tension problem rate dependent solution without damage effects. As seen in the absence of damage development, area reduction during neck development is considerably less. Hence, plastic flow and associated temperature development is smaller. At top, distributions over central plane along plate plane are shown. At the bottom, central transverse section distributions are given. The outer frame denotes the undeformed shape to highlight the amount of deformation by necking. (a) min/max $\alpha = 1.571 \times 10^{-1}/3.291 \times 10^{-1}$, (b) min/max $\Theta = 306.1/326.6$ K.

The load–displacement and the central temperature increment history plots are given in Fig. 8a and b, respectively. It is seen that the models for which convective heat transfer from the surface is accounted for show a relatively rapid decrease in force response after the peak which signals the development of the neck. With damage coupling, a considerable softening is observable. Temperature development at central section of the specimen for the case with damage coupling and heat convection is given in Fig. 8b. In agreement with the thermally triggered necking results given in Simó and Miehe (1992), the maximal temperature difference in the specimen rapidly increases with the development of the neck at which the deformation as well as self-heating with dissipative inelastic processes are localized. At the specimen ends, on the other hand, the temperature remains approximately constant also dictated by the surface heat convection.

Fig. 9 depicts the temperature development during loading whereas in Figs. 10 and 11 corresponding damage and hardening strain-like variable evolutions are given. Unlike the homogeneous solution for which the specimen section remains rectangular along the specimen length, the deformed cross section in the necked zone exhibits double curvature: concave in direction of the width and convex in direction of the thickness in agreement with Simó and Miehe (1992). Thus, although in the homogeneous case the stress triaxiality ratio remains as 1/3, as a result of the curvature development three-dimensional state of stress prevails at the central section. This in turn results in amplified damage accumulation and subsequent local failure, i.e., locally damage reaches 1. For the homogeneous solution, the damage magnitude at $\Delta u = 2 \times 5.96$ mm is only $D = 5.259 \times 10^{-2}$ which is far from critical. At the same deformation level the temperature and

hardening development on the other hand are 317.9 K and $\alpha = 1.978 \times 10^{-1}$, respectively. Since heat convection through surface is not allowed, there occurs no temperature gradients and hence the homogeneous solution is equivalent to an adiabatic analysis.

Finally, Fig. 12 shows temperature and strain hardening variable contour plots, damage uncoupled case. In the absence of damage, this localized deformation problem is transformed into a diffuse necking problem where the reduction of the central area is less than that of damage coupled analysis. Also the development of temperature as well as plastic flow is noticeably smaller than those occurring in a damage coupled analysis.

6. Closure

In this work, an extension of Simó and Miehe (1992) and its followup works (Armero and Simó, 1993a,b) to rate dependent damage-coupled thermomechanics are proposed. It is shown that, once the extensive property of the entropy is exploited, together with a temperature dependent damage dissipation potential, its decomposition into elastic, viscoplastic and damage parts is possible, with corresponding structural changes. Besides it is shown that in addition to those mutual interactions of the mechanical and thermal fields presented in Simó and Miehe (1992), there exist damage induced effects on thermal and other mechanical fields. The framework utilizes a principal axes formulation where the stresses are derived utilizing a hyperelastic potential quadratic elastic Hencky strains. This supplies handiness in derivations and implementation of the framework. The resulting thermomechanical problem is solved for a staggered approach with the isothermal split. The derived forms are implemented as ABAQUS `UMAT` and `UMATH` subroutines and utilized in a set of example problems involving geometrical imperfection triggered necking of an axisymmetric bar and thermally triggered necking of a 3D rectangular bar. The first problem reveals that, for a quasi-static analysis, doubly softening mechanism is prone to the problem of spurious mesh dependence due to the loss of ellipticity of the initial boundary value problem. Especially, in the absence of rate effects the mesh dependence is higher whereas inclusion of rate effects acts as a localization limiter. With the second problem, we show that triaxiality increase at the center by necking triggered by surface convection of heat accelerates damage rate considerably and consequently reduces global total strain to failure as compared to the homogeneous analysis without surface heat convection (hence without necking).

Acknowledgment

Financial support provided by the German Science Foundation (DFG) under Contract PAK 250 (TP4) is gratefully acknowledged.

Appendix A. Derivations for the local tangent

Using Eq. (101) and assuming $Y^{\mathrm{d}} - Y_0^{\mathrm{d}} > 0$ the components for the local Jacobian for the simultaneous local integration scheme can be given as

$$\frac{\partial r_1}{\partial \Delta\gamma} = -\frac{2}{3} q^{\triangleleft}(\alpha, \Theta) + 2\mu \frac{1}{1-D} + m\, \kappa^{\mathrm{vp}} \left[\frac{t_\star}{\Delta t}\right]^m \Delta\gamma^{m-1}, \tag{117}$$

$$\frac{\partial r_1}{\partial D} = 2\mu \frac{\Delta\gamma}{[1-D]^2}, \tag{118}$$

$$\frac{\partial r_2}{\partial \Delta\gamma} = -\beta - \Delta\gamma s\, \beta \frac{1}{\langle Y^{\mathrm{d}} - Y_0^{\mathrm{d}}\rangle} \frac{\partial Y^{\mathrm{d}}}{\partial \Delta\gamma}, \tag{119}$$

$$\frac{\partial r_2}{\partial D} = 1 - \Delta\gamma\beta \left[\frac{r}{1-D} + \frac{s}{\langle Y^{\mathrm{d}} - Y_0^{\mathrm{d}}\rangle} \frac{\partial Y^{\mathrm{d}}}{\partial D}\right], \tag{120}$$

where $q^{\triangleleft} = \partial q(\alpha, \Theta)/\partial\alpha$ together with

$$\beta := \frac{1}{[1-D]^r} \left[\frac{\langle Y^{\mathrm{d}} - Y_0^{\mathrm{d}}\rangle}{a(\Theta)}\right]^s \quad \text{and} \quad \frac{\partial r_2}{\partial Y^{\mathrm{d}}} = -\Delta\gamma\, s\, \beta \frac{1}{\langle Y^{\mathrm{d}} - Y_0^{\mathrm{d}}\rangle}. \tag{121}$$

Appendix B. Derivations for the mechanical tangent moduli

Using the viscoplastic/damage correction given in Eq. (96), for a given principal stress component τ_A one has

$$\frac{\partial \tau_A}{\partial \epsilon_B^{\mathrm{e,tri}}} = [1-D]\frac{\partial \tilde{\tau}_A^{\mathrm{tri}}}{\partial \epsilon_B^{\mathrm{e,tri}}} - 2\mu\Delta\gamma\frac{\partial n_A}{\partial \epsilon_B^{\mathrm{e,tri}}}, \quad \frac{\partial \tau_A}{\partial \Delta\gamma} = -2\mu\, n_A \quad \text{and} \quad \frac{\partial \tau_A}{\partial D} = -\tilde{\tau}_A. \tag{123}$$

Using $\delta_{AB}^{\mathrm{dev}} = \delta_{AB} - 1/3$, with δ_{AB} representing the Kronecker delta which is given as

$$\delta_{AB} := \begin{cases} 1 & \text{if } A = B, \\ 0 & \text{otherwise.} \end{cases} \tag{124}$$

Accordingly, using Eq. (54) one can find

$$\frac{\partial \tilde{\tau}_A^{\mathrm{tri}}}{\partial \epsilon_B^{\mathrm{tri}}} = H + 2\mu\delta_{AB}^{\mathrm{dev}} \quad \text{and} \quad \frac{\partial n_A}{\partial \epsilon_B^{\mathrm{tri}}} = \frac{2\mu}{\left\|\tilde{\mathbf{s}}^{\mathrm{tri}}\right\|}\left[\delta_{AB}^{\mathrm{dev}} - n_A\, n_B\right]. \tag{125}$$

Appendix C. Derivations for the thermal tangent modulus

In the view of Eq. (98), for given inelastic dissipation Ω_{mech} using

$$\frac{\partial \Omega_{\mathrm{mech}}}{\partial Y^{\mathrm{d}}} = \frac{\Delta\gamma}{\Delta t}\beta\left[1 + s\frac{Y^{\mathrm{d}}}{\langle Y^{\mathrm{d}} - Y_0^{\mathrm{d}}\rangle}\right], \tag{126}$$

and $q^{\triangleright} = \partial q(\alpha, \Theta)/\partial\Theta$ one has

$$\frac{\partial \Omega_{\mathrm{mech}}}{\partial \Theta} = \frac{\Delta\gamma}{\Delta t}\left[\sqrt{\frac{2}{3}}q^{\triangleright}(\alpha, \Theta) - s\,\beta\, g'_{\omega^{\mathrm{d}}}(\Theta)a_0\frac{Y^{\mathrm{d}}}{a(\Theta)}\right] + \frac{\partial \Omega_{\mathrm{mech}}}{\partial Y^{\mathrm{d}}}\frac{\partial Y^{\mathrm{d}}}{\partial \Theta}, \tag{127}$$

$$\frac{\partial \Omega_{\mathrm{mech}}}{\partial \Delta\gamma} = \frac{\Omega_{\mathrm{mech}}}{\Delta\gamma} + \frac{\Delta\gamma}{\Delta t}\left[\frac{2}{3}q^{\triangleleft}(\alpha, \Theta) - \frac{2\mu}{1-D}\right] + \frac{\partial \Omega_{\mathrm{mech}}}{\partial Y^{\mathrm{d}}}\frac{\partial Y^{\mathrm{d}}}{\partial \Delta\gamma}, \tag{128}$$

$$\frac{\partial \Omega_{\mathrm{mech}}}{\partial D} = -\frac{\Delta\gamma^2}{\Delta t}\frac{2\mu}{[1-D]^2} + r\,\beta\frac{\Delta\gamma}{\Delta t}\frac{Y^{\mathrm{d}}}{1-D} + \frac{\partial \Omega_{\mathrm{mech}}}{\partial Y^{\mathrm{d}}}\frac{\partial Y^{\mathrm{d}}}{\partial D}. \tag{129}$$

For the local tangent, additional derivations include the following:

$$\frac{\partial r_1}{\partial \Theta} = \sqrt{\frac{2}{3}}g'_{\omega^{\mathrm{vp}}}(\Theta)\left[\tau_{y0,0} - q(\alpha, \Theta_0)\right], \tag{130}$$

$$\frac{\partial r_2}{\partial \Theta} = \Delta\gamma\, s\,\beta\left[g'_{\omega^{\mathrm{d}}}(\Theta)\frac{a_0}{a(\Theta)} - \frac{1}{\langle Y^{\mathrm{d}} - Y_0^{\mathrm{d}}\rangle}\frac{\partial Y^{\mathrm{d}}}{\partial \Theta}\right]. \tag{131}$$

Using Eq. (56) we reach

$$\frac{\partial Y^{\mathrm{d}}}{\partial \Theta} = \frac{\partial \tilde{\Psi}^{\Theta\mathrm{e}}(J^{\mathrm{e}}, \Theta)}{\partial \Theta} = -3\,H\,\alpha_\Theta\log(J^{\mathrm{e}}). \tag{132}$$

Using $\partial[\bullet]/\partial\epsilon_B \equiv \partial[\bullet]/\partial\epsilon_B^{\mathrm{e,tri}}$ one reaches

$$\frac{\partial r_1}{\partial \epsilon_B} = -2\mu\, n_B \quad \text{and} \quad \frac{\partial r_2}{\partial \epsilon_B} = -\Delta\gamma\, s\,\beta\frac{1}{Y^{\mathrm{d}}}\frac{\partial Y^{\mathrm{d}}}{\partial \epsilon_B^{\mathrm{e,tri}}} \tag{133}$$

where Eq. (130.1) is computed using $\left\|\tilde{\mathbf{s}}\right\| := [\tilde{s}_1^2 + \tilde{s}_2^2 + \tilde{s}_3^2]^{1/2}$ and

$$\frac{\partial\left\|\tilde{\mathbf{s}}^{\mathrm{tri}}\right\|}{\partial \epsilon_B^{\mathrm{e,tri}}} = 2\mu n_B. \tag{134}$$

Appendix D. Derivations for the plastic dissipation

Using the proposed von Mises yield potential and degree one homogeneity property of the yield potential, one may derive the following equivalence for the plastic part of the dissipation expression:

$$\Omega^{\mathrm{vp}}_{\mathrm{mech}} = \boldsymbol{\tau}\colon\left[-\frac{1}{2}\mathcal{L}_v\mathbf{b}^{\mathrm{e}}\cdot[\mathbf{b}^{\mathrm{e}}]^{-1}\right] + q\,\dot{\alpha} = [1-D]\big[\tilde{\mathbf{s}}+\tilde{p}\mathbf{1}\big]\colon\left[\frac{\dot{\gamma}}{1-D}\frac{\tilde{\mathbf{s}}}{\|\tilde{\mathbf{s}}\|}\right] + q(\alpha,\Theta)\left[\sqrt{\frac{2}{3}}\dot{\gamma}\right] = \dot{\gamma}\left[\|\tilde{\mathbf{s}}\| + \sqrt{\frac{2}{3}}q(\alpha,\Theta)\right] \tag{135}$$

with $\tilde{\boldsymbol{\tau}} = \boldsymbol{\tau}/[1-D]$, $\tilde{\boldsymbol{\tau}} = \tilde{p}\mathbf{1} + \tilde{\mathbf{s}}$ and $\tilde{p}\mathbf{1}\colon\tilde{\mathbf{s}} = 0$, and consequently $[\boldsymbol{\tau}/[1-D]]\colon\tilde{\mathbf{s}} = \tilde{\mathbf{s}}\colon\tilde{\mathbf{s}} = \|\tilde{\mathbf{s}}\|^2$.

Appendix E. Derivations for the damage conjugate variable

Derivation of any of

$$\frac{\partial Y^{\mathrm{d}}}{\partial \epsilon^{\mathrm{e,tri}}_B},\quad \frac{\partial Y^{\mathrm{d}}}{\partial \Delta\gamma}\quad\text{and}\quad \frac{\partial \mathrm{Y}^{\mathrm{d}}}{\partial \mathrm{D}} \tag{136}$$

exploits the chain rule as follows:

$$\frac{\partial Y^{\mathrm{d}}}{\partial[\bullet]} = \frac{\partial Y^{\mathrm{d}}}{\partial J^{\mathrm{e}}}\frac{\partial J^{\mathrm{e}}}{\partial[\bullet]} + \sum_{A=1}^{3}\frac{\partial Y^{\mathrm{d}}}{\partial \bar{\epsilon}^{\mathrm{e}}_A}\frac{\partial \bar{\epsilon}^{\mathrm{e}}_A}{\partial[\bullet]}, \tag{137}$$

where $[\bullet]$ represents one of $\epsilon^{\mathrm{tri}}_{n+1,\,B}$, $\Delta\gamma$ or D. The following relations hold

$$\frac{\partial Y^{\mathrm{d}}}{\partial J^{\mathrm{e}}} = H\frac{\log(J^{\mathrm{e}})}{J^{\mathrm{e}}} - 3\,H\,\alpha_\Theta\big[\Theta-\Theta_0\big]\frac{1}{J^{\mathrm{e}}}\quad\text{and}\quad \frac{\partial \mathrm{Y}^{\mathrm{d}}}{\partial \bar{\epsilon}^{\mathrm{e}}_A} = 2\mu\,\bar{\epsilon}^{\mathrm{e}}_A \tag{138}$$

together with

$$\frac{\partial J^{\mathrm{e}}}{\partial \epsilon^{\mathrm{e,tri}}_B} = J^{\mathrm{e}},\quad \frac{\partial J^{\mathrm{e}}}{\partial \Delta\gamma} = 0\quad\text{and}\quad \frac{\partial J^{\mathrm{e}}}{\partial \mathrm{D}} = 0. \tag{139}$$

Computing the deviator of both sides of Eq. (94) and using the plastic incompressibility one has

$$\bar{\epsilon}^{\mathrm{e}}_A = \bar{\epsilon}^{\mathrm{e,tri}}_A - \frac{\Delta\gamma}{1-D}n_A, \tag{140}$$

with which one may derive

$$\frac{\partial \bar{\epsilon}^{\mathrm{e}}_A}{\partial \epsilon^{\mathrm{e,tri}}_B} = \frac{\partial \bar{\epsilon}^{\mathrm{e,tri}}_A}{\partial \epsilon^{\mathrm{e,tri}}_B} - \frac{\Delta\gamma}{1-D}\frac{\partial n_A}{\partial \epsilon^{\mathrm{e,tri}}_B}, \tag{141}$$

with

$$\frac{\partial \bar{\epsilon}^{\mathrm{e,tri}}_A}{\partial \epsilon^{\mathrm{e,tri}}_B} = \delta^{\mathrm{dev}}_{AB}. \tag{142}$$

Finally, the following identities prove useful:

$$\frac{\partial \bar{\epsilon}^{\mathrm{e}}_A}{\partial D} = -\frac{\Delta\gamma}{[1-D]^2}n_A\quad\text{and}\quad \frac{\partial \bar{\epsilon}^{\mathrm{e}}_A}{\partial \Delta\gamma} = -\frac{1}{1-\mathrm{D}}\mathrm{n}_A. \tag{143}$$

References

Andrade Pires, F.M., de Souza Neto, E.A., Owen, D.R.J., 2004. On the finite element prediction of damage growth and fracture initiation in finitely deforming ductile materials. Comput. Methods Appl. Mech. Eng. 193, 5223–5256.

Armero, F., Simó, J.C., 1993a. A new unconditionally stable fractional step method for non-linear coupled thermomechanical problems. Int. J. Numer. Methods Eng. 35, 737–766.

Armero, F., Simó, J.C., 1993b. A priori stability estimates and unconditionally stable product formula algorithms for nonlinear coupled thermoplasticity. Int. J. Plast. 9, 749–782.

Čanadija, M., Brnić, J., 2004. Associative coupled thermoplasticity at finite strain with temperature-dependent material parameters. Int. J. Plast. 20, 1851–1874.

Coleman, B., Gurtin, M., 1967. Thermodynamics of internal state variables. J. Chem. Phys. 47, 597–613.

da Cunda, L.A.B., Bittencourt, E., Creus, G., 1998. Analysis of ductile damage coupled with thermoplasticity by the FEM. In: Idelsohn, S., Oñate, E., Dvorkin, E. (Eds.), Computational Mechanics New Trends and Applications. CIMNE, Barcelona, Spain, pp. 1–13.

de Souza Neto, E.A., Perić, D., Owen, D.R.J., 2008. Computational Methods for Plasticity: Theory and Applications. John Wiley & Sons Ltd, Chichester, UK.

Ganapathysubramanian, S., Zabaras, N., 2003. Computational design of deformation processes for materials with ductile damage. Comput. Methods Appl. Mech. Eng. 192, 147–183.
Ganczarski, A., 2003. Thermo-damage coupling modelling and applications for creep conditions. In: Skrzypek, J.J., Ganczarski, A.W. (Eds.), Anisotropic Behavior of Damaged Materials. Springer-Verlag, Berlin, Heidelberg, pp. 317–349. (Chapter 10).
Hakansson, P., Wallin, M., Ristinmaa, M., 2006. Thermomechanical response of non-local porous material. Int. J. Plast. 22, 2066–2090.
Hansen, N.R., Schreyer, H.L., 1994. A thermodynamically consistent framework for theories of elastoplasticity coupled with damage. Int. J. Solids Struct. 31, 359–389.
Ibrahimbegović, A., Gharzeddine, F., 1999. Finite deformation plasticity in principal axes: from a manifold to the euclidean setting. Comput. Methods Appl. Mech. Eng. 171, 341–369.
Ju, J.W., 1990. Isotropic and anisotropic damage variables in continuum damage mechanics. J. Eng. Mech. 116, 283–287.
Kachanov, L.M., 1958. Time of the rupture process under creep conditions. Izv. Akad. Nauk. SSR 8, 26–31.
Lee, E.H., 1969. Elastoplastic deformation at finite strains. ASME J. Appl. Mech. 36, 1–6.
Lemaitre, J. 1971. Evaluation of dissipation and damage in metals. In: Proceedings of I.C.M., vol. 1, Kyoto, Japan.
Lemaitre, J., 1996. A Course on Damage Mechanics. Springer-Verlag, Berlin.
Lin, R.C., Brocks, W., Betten, J., 2006. On internal dissipation inequalities and finite strain inelastic constitutive laws: theoretical and numerical comparisons. Int. J. Plast. 22, 1825–1857.
Lämmer, H., Tsakmakis, Ch., 2000. Discussion of coupled elastoplasticity and damage constitutive equations for small and finite deformations. Int. J. Plast. 16, 495–523.
Marsden, J.E., Hughes, T.J.R., 1994. Mathematical Foundations of Elasticity. Dover, New York.
Maugin, G.A., 1992. The Thermomechanics of Plasticity and Fracture. Cambridge University Press, Cambridge.
Miehe, Ch., 1994. Aspects of the formulation and finite element implementation of large strain isotropic elasticity. Int. J. Numer. Methods Eng. 37, 1981–2004.
Miehe, Ch., 1995. A theory of large-strain isotropic thermoplasticity based on metric transformation tensors. Arch. Appl. Mech. 66, 45–64.
Ogden, R.W., 1984. Non-Linear Elastic Deformations. Ellis Horwood Limited, Chichester.
Rabotnov, Y. 1968. Creep rupture. In: Hetenyi, M., Vincenti, W. (Eds.), Applied Mechanics. Proceedings of the 12th International Congress of Applied Mechanics. Springer-Verlag, Berlin, pp. 342–320.
Reckwerth, D., Tsakmakis, Ch., 2003. The principle of generalized energy equivalence in the continuum damage mechanics. In: Hutter, K., Baaser, H. (Eds.), Deformation and Failure in Metallic Materials. Springer-Verlag, Berlin Heidelberg, pp. 381–406.
Saanouni, K., Chaboche, J.L. 2003. Computational damage mechanics: application to metal forming simulation. In: Comprehensive Structural Integrity. Elsevier Ltd., Amsterdam, pp. 319–374 (Chapter 3.06).
de Souza Neto, E.A., Perić, D., 1995. A computational framework for a class of fully coupled models for elastoplastic damage at finite strains with reference to the linearization aspects. Comput. Methods Appl. Mech. Eng. 130, 179–193.
Simó, J.C., Miehe, Ch., 1992. Associative coupled thermoplasticity at finite strains: formulation, numerical analysis and implementation. Comput. Methods Appl. Mech. Eng. 98, 41–104.
Simó, J.C., 1992. Algorithms for multiplicative plasticity that preserve the form of the return mappings of the infinitesimal theory. Comput. Methods Appl. Mech. Eng. 99, 61–112.
Simó, J.C., Ju, J.W., 1989. On continuum damage-elastoplasticity at finite strains. Comput. Mech. 5 (5), 375–400.
Simó, J.C., Taylor, R.L., 1985. Consistent tangent operators for rate-independent elastoplasticity. Comput. Methods Appl. Mech. Eng. 48, 101–118.
Simone, A. 2003. Continuous-Discontinuous Modelling of Failure (Ph.D. thesis). Technische Universiteit Delft.
Soyarslan, C., Tekkaya, A.E., Akyuz, U., 2008. Application of continuum damage mechanics in discontinuous crack formation: forward extrusion Chevron predictions. J. Appl. Math. Mech./Z. Angew. Math. Mech. 88, 436–453.
Soyarslan, C., Turtuk, I.C., Deliktas, B., Bargmann, S. 2016. A thermomechanically consistent constitutive theory for modeling micro-void and/or micro-crack driven failure in metals at finite strains, Int. J. Appl. Mech. 1650009, http://dx.doi.org/10.1142/S1758825116500095.
Steinmann, P., Miehe, Ch., Stein, E., 1994. Comparison of different finite deformation inelastic damage models within multiplicative elastoplasticity for ductile material. Comput. Mech. 13, 458–474.
Wang, W.M., Sluys, L.J., de Borst, R., 1997. Viscoplasticity for instabilities due to strain softening and strain-rate softening. Int. J. Numer. Methods Eng. 40, 3839–3864.
Weber, G., Anand, L., 1990. Finite deformation constitutive equations and a time integration procedure for isotropic, hyperelastic-viscoplastic solids. Comput. Methods Appl. Mech. Eng. 79, 173–202.
Wriggers, P., Miehe, Ch., Kleiber, C., Simó, J., 1992. On the coupled thermodynamic treatment of necking problems via finite element methods. Int. J. Numer. Methods Eng. 33, 869–883.